Corrosion Study of Silver Nanowires

by

Geoffrey Deignan

A thesis

presented to the University of Waterloo

in fulfillment of the

thesis requirement for the degree of

Master of Applied Science

in

Electrical and Computer Engineering (Nanotechnology)

Waterloo, Ontario, Canada, 2017

Author's Declaration

I hereby declare that I am the sole author of this thesis. This is a true copy of the thesis, including any required final revisions, as accepted by my examiners.

I understand that my thesis may be made electronically available to the public.

Abstract

Indium tin oxide is a transparent conductive material that is widely used in electronic consumer products such as LCDs, LEDs, OLEDs, touch-screen devices, and diagnostic sensors. However, indium tin oxide is costly to produce and is very brittle, limiting its potential for the next generation of flexible and wearable devices and diagnostic tools. Silver nanowires are cylindrically shaped nanostructures that have been touted as the replacement to indium tin oxide. Their electronic performance and transparency outperforms the incumbent technology, and their mechanical flexibility and low implementation costs provide a significant advantage over indium tin oxide for use in electronic applications. However, silver nanowires are unstable and the electrodes can become non-conductive under ambient conditions in less than sixty days. Although silver nanowire degradation is a major problem, few studies exist revealing the challenges with appropriate solutions for enhancing the silver nanowire lifetimes. Through this present work, we found that variables such as nanowire diameter, nanowire density, and pre- and post-deposition processing parameters have a significant impact on the lifetime of nanowire electrodes. These results will be presented and guidelines for improving nanowire stability and lifetime will be outlined.

Furthermore, investigations into an effective conductive organic passivation layer were systematically performed to determine the material's viability as a method of passivating corrosion in the silver nanowire electrodes. It was observed that the organic passivation material was ineffective as a method of preventing corrosion in silver nanowires. In fact, the use of this organic material appears to have caused corrosion to occur at a faster rate than a bare silver nanowire transparent electrode would undergo when exposed to ambient conditions.

Acknowledgements

I would like to thank Dr. Irene Goldthorpe for her guidance throughout the project, and for being a supportive throughout the entirety of my Masters degree. Without her guidance this work would have never been possible. I would also like to thank Dr. Marwa Abd-Ellah for her guidance over the past few months.

I would also like to thank my lab mates and friends- Hadi, Jianjin, Jon, Nupur, Alexandra, Mina, Sue, Koen, and Min for their support in the lab, their valuable discussions, and contributions to this project.

I would also like to thank my family and friends for their constant support throughout the previous two years.

Dedication

I hereby dedicate this thesis to my Mom, Dad, and Rachel.

Table of Contents

List of Figures

List of Tables

List of Abbreviations

AgNW: Silver Nanowire

ITO: Indium Tin Oxide

LED: Light Emitting Diode

OLED: Organic Light Emitting Diode

LCD: Liquid Crystal Display

PET: Polyethylene terephthalate

PVP: Polyvinylpyrrolidone

SEM: Scanning Electron Microscope

TEM: Transmission Electron Microscope

EDS: Energy Dispersive X-Ray Spectroscopy

PCAT: Phenyl Capped Aniline Tetramer

SERS: Surface Enhanced Raman Spectroscopy

FFT: Fast Fourier Transform

Chapter 1:   Introduction

1.1.Transparent Conductive Electrodes

What do the Apple iPhone, Amazon Kindle, Samsung Liquid Crystal Displays (LCDs), Sony Organic Light Emitting Diodes (OLEDs), Nintendo Dual Screens, and Nanosolar solar cells have in common? Each of these disparate devices uses a material that is transparent to visible light and yet electrically conductive as an essential element in the device stack. These so called transparent electrodes are used when a situation calls for low resistance electrical contacts that do not block visible light from entering or leaving the device. Figure 1-2 shows a typical schematic of an LED or OLED with a transparent electrode in its architecture.

Over the last decade there has been a persistent increase in devices, which require one, or more transparent conducting layers, and that trend is forecast to continue for the foreseeable future. Currently, LCDs are by far the largest users of transparent conductive materials, but many other devices are showing rapid growth in popularity such as touch panels (362 million units in 2010 with annual growth of 20% through 2013), E-paper (30 fold growth expected from 2008 to 2014), thin film solar (expected sales of over $13 billion by 2017), and flexible displays [1]. As such, it is forecasted that the transparent electrode market will grow to approximately $5.1 billion by 2020, from $1.9 billion in 2012. In the display segment, flexible displays are expected to make up 11 percent of the market by 2019 [2].
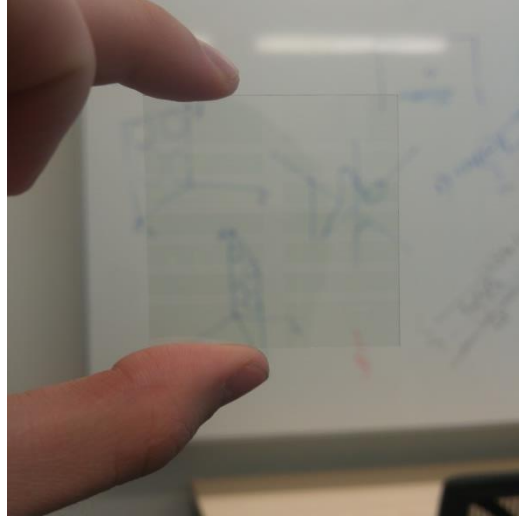
Figure 1-1: Transparent conductive material on glass slide
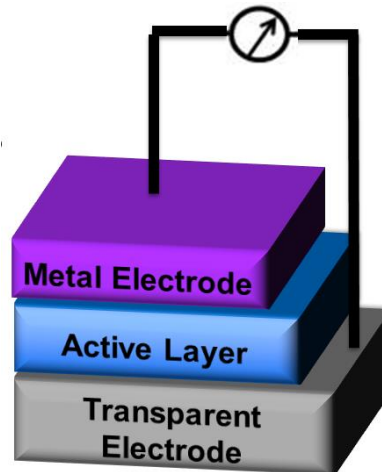
Figure 1-2: Schematic of a typical optoelectronic device structure that uses a transparent electrode material.

1.2. Common Transparent Conducting Materials

The majority of scientific studies and market-available technologies rely on vacuum

processes and transparent conductive oxides (TCOs) such as indium tin oxide (ITO), fluorine

doped tin oxide (FTO) or aluminium-doped zinc oxide (AZO) thin films. These semiconductor

TCOs are transparent to visible light due to the energies of their band gaps being higher than the

energies of photons in the visible range. The transparency of TCOs is controllable due to the ease

of variance in film thickness (thicker films result in a more conductive oxide, but a film of lower transparency) [3]. ITO in particular is widely used as a transparent electrode material because of its high conductivity and controllable properties via its deposition method [4] [5]. ITO has been the backbone of the transparent conducting film market, as most modern display technologies use ITO as a transparent conductor.

Coming generations of optoelectronic devices will require transparent conducting electrodes (TCEs) to be lightweight, mechanically flexible, compatible with large scale processing (such as reel-to-reel), and inexpensive. These new requirements significantly limit the use of TCOs as a conducting medium. This is firstly because they suffer from high fabrication costs due to the need for high vacuum and high temperatures during their deposition, which is usually done by sputtering. Secondly, TCOs are brittle and their conductivity significantly and irreversibly reduces upon mechanical bending [6] [4]. Although researchers have developed a process to evaporate and laminate ITO films onto flexible polyethylene terephthalate (PET) substrates [11], they still crack when flexed to a large degree and additional costs and processing are incurred. Thirdly, indium is a rare and expensive element that is obtained as a by-product of ores mined for their content of other metals such as zinc and lead. There are no "indium mines" because its concentration in minerals is too low to allow economic extraction only for the value of the indium. Thus the supply of indium cannot be increased significantly without a large increase in price sufficient to make "indium mines" profitable [7]. The high cost of ITO deposition, indium scarcity, and film brittleness are prompting the search for replacement materials for the coming generations of transparent conductive materials [6] [4].

1.3.Alternative Transparent Conducting Materials

Numerous alternative transparent electrode materials such as networks of carbon nanotubes (CNTs) [8] [9] [10], metal gratings [11], graphene [12] [13] [14], conducting polymers [4], and metallic nanowire networks [15] are under consideration to be replacements of ITO films in the next generation of electronic devices. A comparison of alternative transparent conductive materials is listed in Figure 1-3. The most popular solutions are summarized in the following subsections.
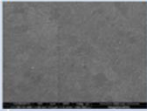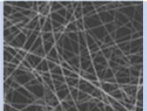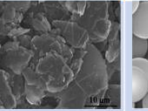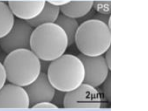
	ITO	Nanowires	Metal Grid	FTO/AZO	Graphene	PEDOT:PSS
Pros	• Well established • 20-100 ohms/sq	• Low cost solution process • Scalable • Flexible	• Highly conductive (<1 - 50 ohms/sq)	• 10-20 ohms/sq • Compatible with glass production	• 300-800 ohms/sq • Possibly solution processed	• <1 kohm/sq • Solution processable
Challenges	• Limited conductivity, especially on plastic • Not flexible • Expensive vacuum process	• 5 ohms/sq with >90% transparency	• Optically visible large openings • Charge spreading • Expensive fabrication process	• Not flexible • Expensive vacuum process	• Sheets must be overlapping • Achieving high transparency with low sheet resistance	• Lifetime issues • Not conductive enough for transparent electrode applications

Figure 1-3: Comparison between proposed transparent conductive materials including benefits and challenges to each listed material [16]

1.3.1. Carbon Nanotubes

Carbon nanotubes (CNTs) have very high electrical conductivity, transparency, flexibility, and a high Young's modulus [17]. These properties make CNTs attractive as a possible replacement to ITO. Transparent electrodes can be fabricated by depositing a film or mesh of CNTs, typically using solution deposition processes such as spin coating, drop casting, or Mayer rod coating [18]. If the density of CNTs is high enough, current can flow from one end

of the film to the other through the connected network of tubes. The films are transparent is achieved by the CNTs because CNTs do not reflect light, but they do not absorb a significant amount of it either [19], allowing light transmission through the remaining 90-95% of the substrate.

There are, however, barriers that CNT researchers must address in order to allow for successful adoption of the technology. Firstly, although the conductivity of an individual CNT is very high, there is high junction resistance between overlapping CNTs that causes the sheet resistance of the overall network to be high. Secondly, the synthesis of CNTs results in both metallic and semiconducting tubes. The latter do not contribute much to conduction but lower the films' transparency. These two factors result in the conductivity being too low at a given transparency for the majority of applications requiring transparent electrodes.

1.3.2. Conductive Polymers

Conductive polymers can be used to fabricate alternative transparent conducting materials to ITO. Poly(3,4-ethylenedioxythiophene) is often combined with poly(styrenesulfonate) (PEDOT:PSS) in order to enable aqueous solubility and thus allow solution processing of the layer [20]. Conductivity across the polymer is achieved via PEDOT rich chains forming in the layer. The use of a polymeric material as a transparent electrode gives the advantage of flexibility and solution processing techniques that are not currently available with ITO electrodes. Conductive polymers have high resistance values at a given transparency however and cannot compete with ITO on these specifications. Other challenges include their stability in water and substrate adhesion [21].

1.3.3. Graphene

Graphene, a two dimensional single-atom-thick carbon lattice, has been regarded as an ideal candidate material to substitute for ITO for the preparation of transparent electrodes as it possesses an especially high electron mobility (>15000 cm^2 Vs^-1) and high optical transmittance (~97.7% for single-layer graphene), in addition to superior mechanical strength, outstanding chemical stability, and high thermal conductivity (~5.0x10^3 W/mK) [22].

Although graphene is widely researched, there are many challenges it must overcome. Although the chemical vapour deposition of layers of graphene leads to low sheet resistances at a given conductivity, the manufacturing cost is not competitive with ITO. A much less expensive conductive film can instead be formed from graphene flakes, but there is a high contact resistance between overlapping flakes leading to a high sheet resistance across the electrode [23]. Although graphene transparent electrodes have promise, they have so far been unsuccessful as an ITO replacement.

1.3.4. Fine Metal Mesh Electrodes

Silver, copper, and gold are among the most conductive elements on the periodic table. However, metals do not possess light transparency like ITO, graphene, or CNT networks and are in fact often used as reflective anodes in LEDs, OLEDs and display devices. The advent of lithography-processed fine metal mesh grids of these conductive metals does allow for metals to be used as transparent electrode materials [24, 25, 26]. Fine metal mesh grids are periodic grid structures consisting of wires with diameters less than 100 nm, and periods around 500 nm (Figure 1-4). They allow for easy electron flow between each column and row, while allowing light to pass in the space between the wires. Electrodes fabricated using these methods have

sheet resistances of 6.5 Ω/□ at a transparency of 91%, which is an improvement in both

conductivity and transparency over CNTs, graphene, conductive polymers, and ITO [26].
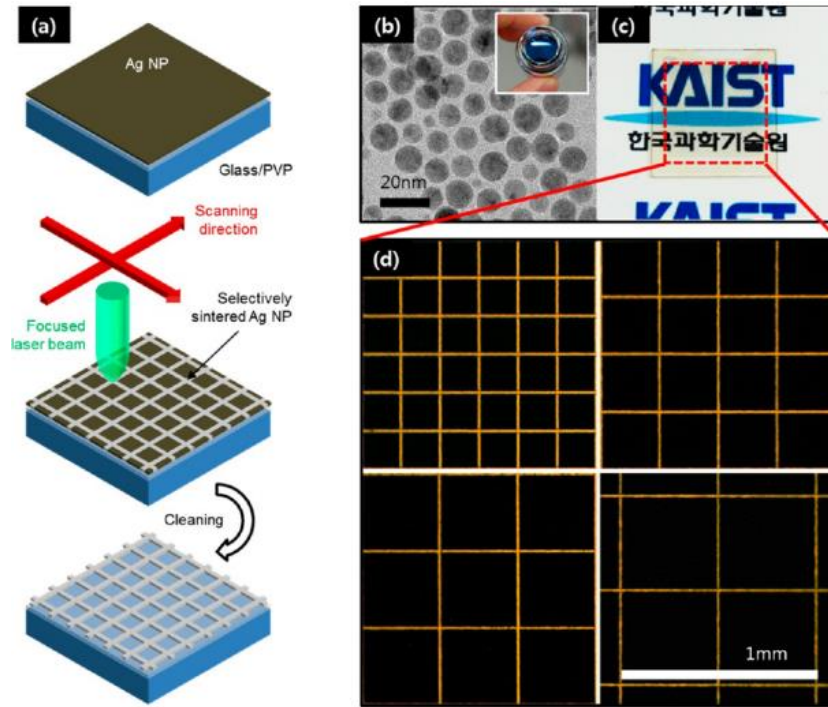
Figure 1-4: (a) Schematic diagram of selective laser sintering of silver nanoparticles for the fabrication of a transparent conductor. (b) Transmission electron microscopy image of synthesized silver nanoparticle ink (inset: optical photograph of ink). (c) Photograph of a transparent conductor on a glass substrate (metallic grid in the red-boxed region). (d) Optical stereoscope image of square-metallic grids at different grid sizes (200 to 500 μm, increment 100 μm) [25].

Although low sheet resistances and high transparency are achievable metrics with fine

metal mesh electrodes, the amount of processing required to lithographically produce these

metallic grids with mesh thicknesses of 45-100 nm is significant [26]. Furthermore, the use of

thermal evaporation techniques adds to the fabrication cost of the electrode. These heavy

processing steps and high cost are major drawbacks to using fine metal mesh grids as transparent

electrodes.

1.4.Silver Nanowire Networks

Recent interest in silver nanowires (AgNWs) has proliferated due to their ability to replace incumbent transparent conductive oxides such as indium tin oxide (ITO) in electronic devices. AgNWs have been materials of interest specifically for the replacement of ITO films since Xia et al first demonstrated their easy and inexpensive synthesis via the polyol method [27]. AgNWs are synthesized in solution and then can be deposited as films onto substrates such as glass or plastic via slot die coating, spin coating, Mayer rod coating, or drop casting [27]. After their deposition using a variety of methods, a random mesh of AgNWs is formed on the substrate surface, from which current can flow because of the overlapping AgNWs.

Silver nanowire networks are transparent because of the minimal surface coverage that the AgNWs take on the substrate. The surface coverage of the AgNWs on the surface of the substrate can be anywhere between 5-15% (Figure 1-5). Although the AgNWs will reflect and refract light [28], between 85-95% of all light will transmit through the substrate.
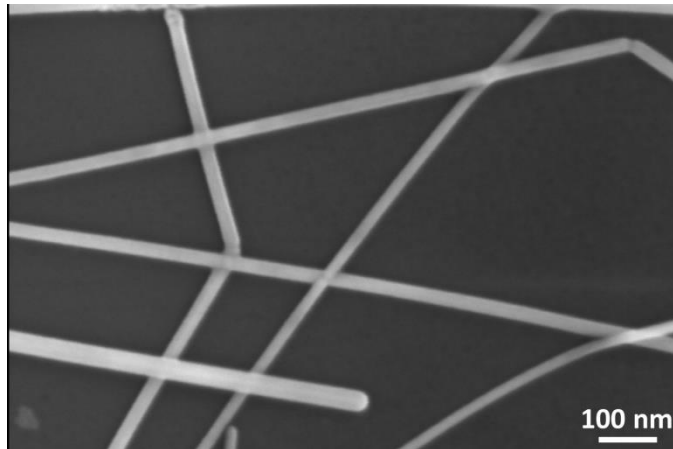
Figure 1-5: Silver nanowire network on a silicon substrate.

Silver nanowire films are usually considered to be a better replacement to ITO than CNTs because of their higher conductivity. This is because unlike batches of CNTs where there is generally a mix of metallic and semiconducting tubes, all silver nanowires are metallic. Also,

overlapping CNTs suffer from high junction resistances, while AgNWs can have junctions

welded or sintered together which greatly reduces junction resistance [6]. AgNWs are preferred

to materials such as graphene and fine metal meshes as well because of the low cost of synthesis

and deposition as compared to CVD-deposited graphene and metal mesh electrodes. When

correlating transparency to sheet resistance, AgNW films outperform all of these other materials

(Figure 1-6) [6]. Based on both cost and performance analyses performed by Emmott et al and

Lee et al., AgNW based transparent electrodes appear to be the most suitable alternative to TCO

films [29] [30].
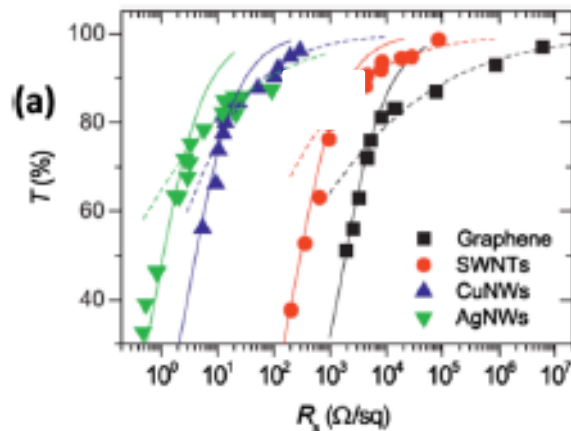
Figure 1-6: Comparison between transparent electrode performance and optical transmittance at 550 nm of transparent conducting materials. [31].

AgNW-based electrodes are already being used in commercial touchscreen devices [19],

and have also been shown to be candidates for solar applications [32] [33] [34] [35], transparent

heaters [36], OLED displays [37] [38] [39], touch panels [40], smart windows [41], and sensors

[42] [43] [44]. Furthermore, AgNW networks have recently been demonstrated for other

applications that are discussed in the following subsection.

1.4.1. *Applications of Silver Nanowires*

Although transparent conductive electrodes have been listed as the main application of

AgNWs, there are many different published works that use AgNWs as the active component in a

variety of other applications, such as biocompatible devices, transparent inks, and transparent heaters.

In recent decades, biocompatible polymers have become wide-spread materials in medicinal technology. However, it was found that there is a risk associated with their application; their long-term use often leads to bacterial colonisation, biofilm formation and development of hospital-acquired infections. Researchers have realized the use of AgNWs as antimicrobial materials, as they have significant antimicrobial properties and have the ability to break cell walls [45]. For this reason, AgNWs have been explored as a disinfectant surface material for a variety of applications [46] [47]. Furthermore, AgNW materials have been used as flexible antennas in biocompatible devices [48] [49].

AgNWs have been envisioned as transparent inks for smart clothing and textiles. The ability to change the colour of a garment [50], act as a transparent heater for textiles and clothing [51], or use an active bio-monitor to measure athletic performance has been an area of heavy research for AgNW based fabrics [52] [53]. AgNWs have also been used as the active component in electrochromic devices, [54] [55] [56] and have been explored for use as transparent heaters for applications such as aerospace and clothing [57] [58]

Therefore, although this thesis assumes transparent electrodes as the application for AgNW films, the results of this thesis will be useful for many other applications as AgNW degradation will affect most or all of the applications mentioned above.

1.4.2. *Synthesis of Silver Nanowires*

Batch synthesis of AgNWs was first reported by Xia et al in 2002 via the polyol method in which ethylene glycol is used to reduce the metal precursor (usually silver nitrate) in the

presence of a nucleating agent and polyvinylpyrrolidone (PVP) [27]. Silver nanowires

synthesized via polyol method have been used to create transparent electrodes with

transparencies over 90% and sheet resistances below 10 $\Omega/\square$.

Silver nanowires synthesized via the polyol process follows the schematic listed in Figure

1-7 [59]. Silver nitrate is reduced by ethylene glycol in the presence of the polymer poly (vinyl

pyrrolidone) (PVP). Silver or platinum seed particles of a few nanometers are commonly used,

but formation of Ag seeds from the reduction of silver nitrate ($AgNO_3$) into Ag^+ in ethylene

glycol is becoming a more preferred method. In a typical synthesis process (according to Coskun

et al) [60], the reduction of silver nitrate into silver ions is achieved when $AgNO_3$ dissolves into

ethylene glycol with PVP and sodium chloride (NaCl). Silver nanoparticles form quickly, with

silver nanowires growing after the reaction proceeds further. The incorporation of PVP into the

mixture aids in anisotropic growth in the {110} direction [60] [61]. The growth mechanism of

AgNWs is illustrated in Figure 1-7 [59].
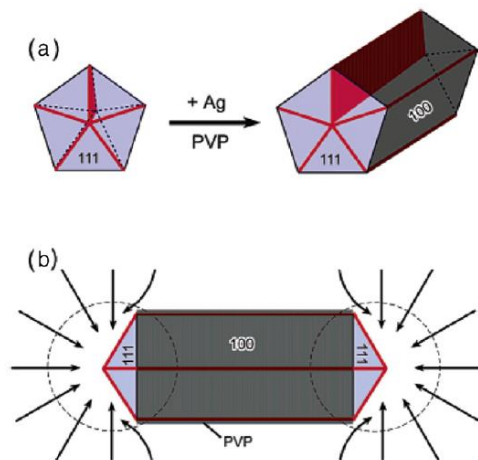
Figure 1-7: Illustration of the mechanism proposed to account for the growth of AgNWs through the polyol process. (a) Evolution of a multiply-twinned nanoparticle of silver to a silver nanowire. (b) The diffusion of silver atoms towards the two ends of a nanorod, with the side surface being completely passivated by polyvinylpyrrolidone [59].

1.4.3. Silver Nanowire Degradation

Although AgNWs appear to be the next miracle material, poised to displace ITO in the transparent electrode market, the material still has drawbacks associated with its use. For example, AgNWs suffer from challenges associated with surface roughness (addressed via hot-rolling by Khaligh et al) [62], and their electrical instability if electrical currents are sustained over long times [63]. Many of these issues have or can be solved, but the largest obstacle to the use of AgNWs as transparent electrodes remains related to the longevity of the material [68 - 72]. Because AgNWs are thinner than 100 nm, as well as have very high surface area to volume ratios due to their shape and small diameter, instability and corrosion are severe problems. AgNWs have been known to become discontinuous when left in atmospheric conditions for less than 6 months [64], which leads to electrode failure. Atmospheric corrosion of bulk and thin-films of silver is a relatively known subject, but far less is known about the stability and degradation of silver nanowires. The few studies on this latter topic focus on the environmental conditions nanowires are exposed to. Humidity [65], elevated temperatures [66], light exposure [22], and high electrical currents [63] are all known to accelerate AgNW degradation. However, these factors alone cannot explain why silver nanowires and nanowire electrodes prepared by different groups have vastly different lifetimes. Silver nanowires prepared by Mayousse et al. [67] are reported to be stable when stored in ambient atmosphere for up to two and a half years, while AgNWs prepared by Elechiguerra et al. [64] and Jiu et al. [68] degrade to the point of non-continuity in as little as 30 days under similar conditions. In the context of transparent electrodes, Mayousse's samples showed a minimal sheet resistance increase in 2.5 years, while the electrodes prepared in two other studies, one by Jiu and the other by Vaagensmith [27], were non-conductive via open circuit in less than 6 months. Moon also discussed nanowire corrosion

in some detail, finding that the resistance of electrodes increased approximately 250% over a time period of 2 months [69]. In all these works, the AgNWs were similarly synthesized using the polyol method and it is unclear why their rates of degradation differed. It is important to determine what factors affect silver nanowire degradation so lifetimes can be increased. Others have studied environmental factors, but not the composition of the NW film itself or the procedures used to process the NW films into electrodes.

1.6. Corrosion of Bulk Silver

The corrosion of silver nanowires specifically has not been studied in detail, but it is helpful to review what is known about the corrosion of bulk silver. Unlike other metals, silver does not naturally forms a surface oxide. Exposure to reduced sulfur compounds produces a film of silver sulfide (Ag_2S). Long exposures produce small amounts of a second component, which may be either silver oxide (Ag_2O) or silver sulfate (Ag_2SO_4). In contrast to its reactivity with reduced sulfur compounds, the sulfidation of silver by sulfur dioxide (SO_2) is very slow. The most abundant sulfur compound present in atmospheric concentrations is carbonyl sulfide (OCS), with the next most abundant gas being SO_2. H_2S and any other flowers of sulfur are rarely present in the atmosphere [70]. Franey et al. exposed bulk silver coupons to H_2S, OCS, CS_2 and SO_2 gases to observe kinetic data on their corrosive properties over a varied time span. As such, the time required to form a 5 nm film thickness of Ag_2S film on these bulk coupons is listed in Table 1-1.

Table 1-1: Time required forming a 5 nm thick Ag_2S film in the ambient atmosphere [70]

Corrosive Gas	Exposure to form film (ppb h^{-1})	Ambient Concentration (ppb)		Time to form 5 nm film (days)	
		Near source	Background	Near source	Background
H_2S	10^2	5	0.03	1	140
OCS	10^3	0.5	0.5	80	80
CS_2	$>10^7$	0.3	0.03	$> 7 \times 10^6$	$> 7 \times 10^7$
SO_2	7×10^8	100	0.1	3×10^3	3×10^7

Below are the film thicknesses of studied gases at a range of different temperatures. The plots show the dependence of sulfur absorption on the silver surface as a function of temperature.
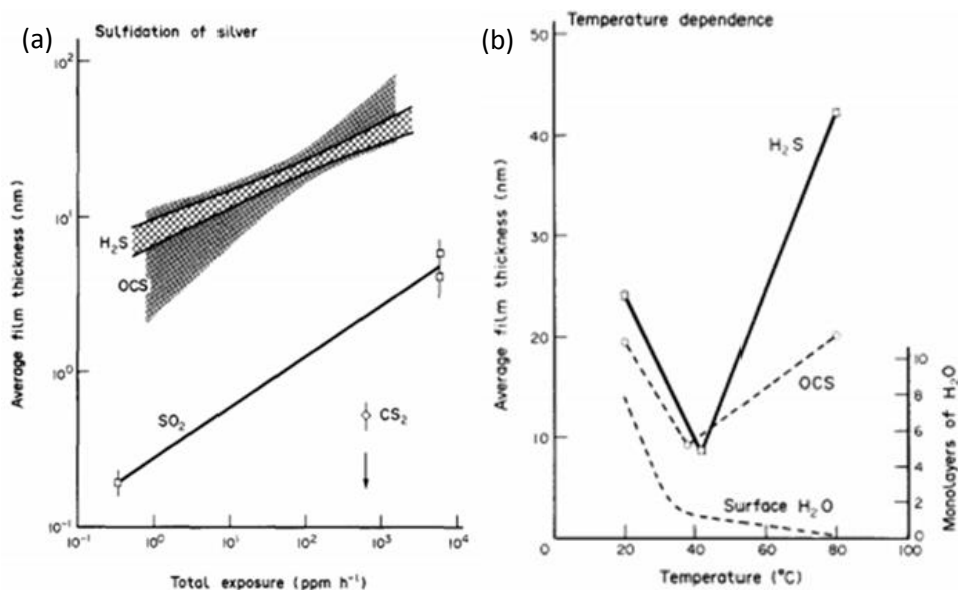
Figure 1-8: Growth rates of Ag₂S when exposed to various ambient sulfur-containing gases. (a) The thickness of Ag₂S corrosion film as a function of total exposure to H₂S, OCS, SO₂ and CS₂. (b) Ag₂S film thicknesses at total exposures of 100 ppm h-1 H₂S or OCS, as a function of temperature [70].

During this investigation, Franey concluded that SO_2 and CS_2, despite being highly prevalent in the atmosphere (in comparison to H_2S and OCS), have very little-to-no effect on corroding bulk silver ingots. Atmospheric gases directly contributing to corrosion of the silver surfaces listed were H_2S and OCS, as dictated by Figure 1-8. Franey also concluded that conditions such as humidity and temperature have a significant effect on corrosion rates, as higher humidity and higher temperature result in faster formations of Ag_2S [70]. Graedel also reported on the increased rate of corrosion on silver in humid environments.

The growth of tarnish on silver films has been further identified to be exclusively growths of Ag_2S [71]. Bennett et al reported Ag_2S tarnish growth site densities of about $4 \times 10^{11} cm^{-2}$, which are comparable with densities noted by Franey. In an experiment designed to measure the

14

relative chemical activities of various planes, facets, and steps on thermally etched polycrystalline silver films that had been artificially tarnished in a sulfur-rich atmosphere, they noted two different silver morphologies. On atomically smooth planes, the least active were the {111} planes on which they observed small, slow growing, irregularly shaped, randomly spaced clumps of silver sulfide. However, on the more chemically active surfaces, those with high indices, slip surfaces, or complex facets, they observed large, fast-growing, angular patches of silver sulfide with a site density of about $3 \times 10^9 \text{cm}^{-2}$, two orders-of-magnitude less than for the chemically inactive surfaces. They attributed the differences in chemical activity of the various surfaces to differences in the silver-silver binding energies. Silver atoms in the close-packed {111} planes are tightly bound, and therefore are least likely to escape their positions in the lattice and react with the sulfur [71].

Silver plating is widely used on contacts and other conductive parts in electrical apparatus such as switchgear and motor control centers because of the superior conductivity and longevity. The silver is found on the bus, in the circuit breaker, in protective relays, auxiliary relays, control switches, and test switches. The decomposition of the contact surfaces leads to an increase of the contact resistance and consequently to a rise in temperature, and eventually to the failure of the component [72]. The growth of Ag_2S on Ag components in electronic circuits can alter the conductivity of silver due to the semiconducting nature of Ag_2S, and can even lead to short circuiting due to bridging of the Ag_2S between silver contact pads [73]. Silver corrosion results in a high resistance, which produces more heat, which in turn stimulates the further tarnishing and the growth of Ag_2S. This process continues and leads to the failure due to overheating or short circuit [73].

1.7. Silver Nanowire Corrosion and Passivation Strategies

There exists a few works stating that AgNWs readily corrode in ambient conditions, and somewhat explain what occurs after a short period of atmospheric exposure [64] [74]. Elechiguerra stated in his work that a thin shell of Ag_2S could be observed on the surface of the AgNWs analyzed. This was confirmed in his report using EDS and Surface Enhanced Raman Spectroscopy (SERS) [64]. Vaagensmith and Mayousse also briefly discussed this, but this was stated after exposure to conditions with relatively high humidity and temperature (as well as exposure to light) [70] [74]. Light exposure has been briefly addressed as a factor that affects corrosion rate, but once again, there is little-to-no explanation as to the mechanisms behind the corrosion of AgNW electrodes [65] [64]. The general consensus amongst the scientific community appears to be the acceptance that AgNWs corrode based on formation of Ag_2S on their surface. There are papers that address the environmental factors that affect AgNW corrosion, but there are no reported works that address how the physical properties of AgNW electrodes, or typical processes that are used to fabricate AgNW electrodes, affect corrosion rates.

There have been some attempts at mitigating corrosion in AgNW networks using a variety of materials. Materials such as thermally evaporated Ni [75], TiO_2 [76], ZnO [77], graphene [78, 79], and CNTs [80] have been demonstrated as potential passivation layers for AgNW electrodes. Each of these materials shows that some resistance to corrosion can be achieved, but there are still increases in sheet resistance over an extended period in all of these reported works. Furthermore, thermally evaporated core-shell structures and CVD core-shell structures (such as an Ag/Ni shell structure [75], and CNTs grown along the outside of the AgNW [80]) require time-consuming processing methods. Also, all of the materials researched

as passivation layers had a detrimental effect on either the transparency (nickel, graphene, CNTs), or sheet resistance (TiO_2 and ZnO). Therefore, these materials are only partial solutions to the overarching problem of AgNW corrosion. There still remains the open issue of finding a passivation layer for AgNWs that does not affect the transparency or sheet resistance while acting as a complete barrier to corrosion. If a barrier exists for AgNWs that is 100% effective in preventing corrosion, does not have any detrimental effect on sheet resistance or transparency of the electrode, and still allows for integration with various devices (such as OLEDs, LEDs, or solar cells), only then would AgNWs be considered an effective replacement to ITO.

1.8. Thesis Organization

It is important to determine why and how the nanowire film itself affects lifetime to be able to improve passivation technologies to improve longevity. In this work, it is studied for the first time, how the electrode composition and common processing parameters used to fabricate AgNW electrodes affect nanowire stability and electrode lifetimes. Chapter 2 details the fabrication methods used to prepare AgNW electrode films using a variety of different solvents, substrates, nanowire diameters, film densities, and various pre- and post- deposition processing parameters and exposure to atmospheric conditions. Chapter 3 will state the results observed, and reveal valuable information on what variables affect silver nanowire degradation and therefore how to increase the lifetime of silver nanowire materials. Chapter 4 will focus on passivation materials, and new methods proposed to reduce the corrosion rates of AgNWs. Chapter 5 will provide a summary of the results observed, provide strategies to increase electrode lifetime using the information obtained in this thesis, and detail future work that must be done in order to effectively increase the lifetime of AgNW electrodes.

Chapter 2:   Fabrication and Characterization of Silver Nanowire Electrodes

This chapter will first discuss the fabrication process of silver nanowire electrodes using a variety of solvents, substrates, nanowire solution densities, NW lengths, NW storage times, chemical treatments and different strategies to reduce film resistance. Then, the storage methods used to investigate the effect of various parameters on the degradation and lifetime of the nanowires will be described. Finally, this chapter will discuss characterization methods used to determine the sheet resistance, transparency, and extent of corrosion detected in degraded AgNW electrodes.

2.1. Methods of Producing Silver Nanowire Electrodes

In nanowire electrodes, charge is transported through the AgNWs through the transfer of electrons along the AgNWs. Denser nanowire networks are more electrically conductive but less transparent, so different densities are used for different application requirements. AgNWs synthesized using the polyol process can be dispersed in a variety of solvents, and then deposited as films using a variety of solution deposition methods. Demonstrated methods of depositing AgNWs in the literature include spin coating [81, 82], spray-coating [83, 79, 84] vacuum filtration [85], and Mayer bar-coating [86, 87, 88]. In the present work, Mayer rod coating is performed for silver nanowire deposition because it is the most commonly used method used by researchers and industry for depositing NW electrodes, due to its fine control of film thickness capability [89], ease of scalability and large scale production compatibility using roll-to-roll and slot-die coating techniques, which are commonly used in industrial settings. Mayer rod coating is typically performed by rolling or pulling a wire-bound rod across a substrate that is an analogue (albeit at smaller scale) to reel-to-reel coating (Figure 2-1). Film thicknesses of Mayer rod

coatings can be controlled through viscosity and solution density. The more viscous the solution

(or the denser the solution), the thicker the coating will be after the solvent has evaporated [11].
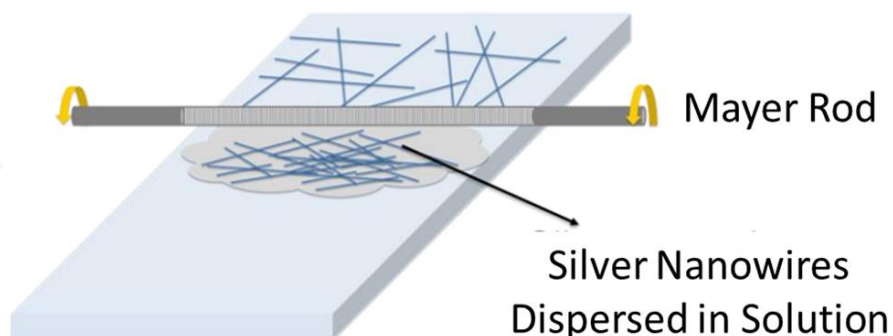
Figure 2-1: Illustration showing the deposition of silver nanowires using the Mayer rod method. Silver nanowires dispersed in a solvent are pipetted across the edge of a substrate, and the Mayer rod is rolled along the length of the substrate to produce a uniform layer with full surface coverage

2.2. Fabrication of Silver Nanowire Electrodes

In order to produce silver nanowire electrodes, different treatment of both the substrate

and NW solution should be considered. Various substrates including polyethylene terephthalate

(PET)(ST505 Melinex film, DuPont Teijin Films), quartz glass and silicon wafers, all having

dimensions of 5 cm x 5 cm (cut to size), were used. The substrates were first sonicated in

isopropyl alcohol (IPA), acetone, and distilled water for 180 seconds in each respective solvent,

and blown dry with a nitrogen gun to ensure removal of dust, organics, and debris that would

interfere with the deposition of the nanowire films. Purchased silver nanowires (Blue Nano 90

nm nanowires, Novarials A20, Novarials A70, Seashell California hi-flex e-ink, ACS Materials

D50, and ACS Materials D70), with average diameters ranging from 20 to 90 nm and average

lengths ranging from 10 to 200 μm were selected to be tested for the series of experiments.

Nanowires were purchased in three different solvents: ethanol, isopropyl alcohol and water. The

nanowire solutions were diluted to their desired concentration (experiment dependent) and re-

dispersed via mechanical agitation to ensure an even distribution of nanowires in solution.

A Mayer rod of size 10 was purchased from R.D. Specialities Inc. (the size of the Mayer rod is related to the thickness of the deposited wet film). A small volume of nanowire solution was pipetted at one end of the desired substrate, and the Mayer rod was slowly rolled to spread the nanowires along the length of the substrate (Figure 2.1) [90, 89, 91]. Measured wet film layers were calculated to be 23 µm in thickness. The coated substrate was then set aside for 3 minutes to allow for solvent evaporation, rotated 90 degrees, and then re-coated using a cleaned Mayer rod. This procedure was repeated two consecutive cycles to ensure a random nanowire mesh coating across the substrate surface for a total of 4 nanowire coatings using the Mayer rod.

Fabricated electrodes were then subject to thermal annealing, mechanical pressing, or no further processing (depending on the experimental parameters being tested). Figure 2.2 shows an example of a fabricated AgNW electrode with junctions formed between the overlapping AgNWs with a fairly uniform network density. Post treatment techniques involving annealing or pressing AgNWs are common methods used to reduce the sheet resistance of AgNW electrodes from $M\Omega/\square$ to a few $\Omega/\square$ [92] [93]. The high junction resistance observed of the overlapping AgNWs is due to the poor contact between the individual nanowires- caused by the polyvinyl pyrrolidone (PVP) outer shell that prevents the direct contact between individual AgNWs. Annealing at a high temperature (between 150-200°C) for a short period of time causes the PVP layer to dissipate, and allows for the AgNWs to weld together at the junction- creating a continuous network of silver [92]. Pressing the AgNWs forces the junctions together due to mechanical pressure- yielding the formation of a highly conductive AgNW network.
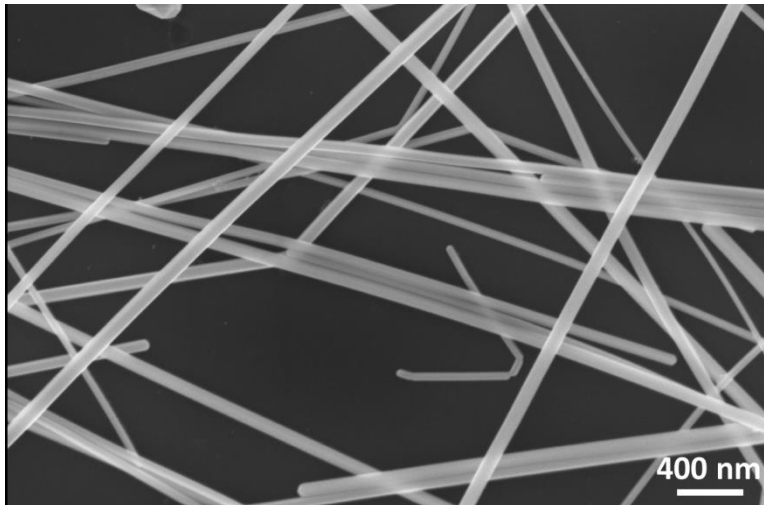
Figure 2-2: Silver nanowire electrodes using Blue Nano 90 nm AgNWs on a silicon substrate fabricated via a Mayer rod coating method

2.2.1. *Thermal Annealing Process:*

Thermal annealing is the most common post-treatment method, which assists in lowering the junction resistance of overlapping nanowires, and causes flowing or partial decomposition of the polyvinylpyrrolidone (PVP) layer that exists on the AgNWs after their polyol synthesis [94, 92, 89, 95]. Annealing of the nanowire electrode involves placing the coated substrate into a vacuum oven at a set temperature (exact temperatures are discussed in chapter 3), and baking the electrode for a set amount of time to allow for the sintering process and decomposition of the PVP coating to take place. To test the impact of the annealing temperature on the long-term stability for 60 days of the nanowires, selected electrodes on glass substrates were annealed in low vacuum at a temperature between 80 - 180°C for 30 minutes [92]. Electrodes on plastic substrates were annealed in low vacuum for 30 minutes at 100°C to prevent any deformation of the plastic.

2.2.2. Mechanical Pressing:

As an alternative to annealing, a different set of electrodes was subjected to room temperature mechanical pressure to lower the nanowire junction resistances [93]. This method was studied, as mechanical pressing is an alternative to lowering the sheet resistance of the AgNW by pressing the nanowire junctions together. This pressing action is preferable to thermal annealing, as it is quicker, and avoids high temperature processing (allowing the use of flexible substrates such as PET) [62]. This method was both used as a comparison to the thermal treatments, and for other samples where different variables (nanowire diameter, density, etc.) were tested to separate their effects from those caused by annealing. A rolling press (MSK-HRP-01, MTI Corporation, Richmond, USA) with a rolling speed of 5 mm/s was used. Electrodes were pressed four times, two times with the two rollers spaced 70 μm apart, and then a subsequent two times with a roller spacing of 60 μm.

2.2.3. Corona Plasma Treatment:

Corona plasma is a common surface treatment using radio frequency (RF) plasma that creates a hydrophilic surface for enhanced material adhesion on the substrate [96]. In a different set of experiments, following the substrate-cleaning step, a corona plasma treatment was performed on glass and PET, via a SoftLithoBox (BlackHole Lab, Paris) [97]. The tip was held 1 cm above the surface of the substrate to allow for electrical discharge to reach the surface. The tip was passed over the substrate five times to ensure a full treatment of corona plasma. Plasma-treated substrates were immediately coated with nanowires in the method listed above. No additional treatments such as pressing or annealing were involved in this set of experiments.

2.2.4. Electrode Characterization

The two most critical characteristics of a transparent electrode are its sheet resistance and transparency. Electrode sheet resistances were measured via a digital multimeter (V&A Instruments VA18B). Their specular transparencies were recorded with a spectrophotometer (SRW 2000 Window Tint Meter), and the contribution of the substrate was subtracted out to obtain the transparency of the NW film only. Scanning electron microscope (SEM) micrographs were taken with a LEO 1550 GEMINI system. Non-conductive samples were coated with 10 nm of gold to prevent surface charging effects. Energy dispersive X-ray spectroscopy (EDS) was performed in the SEM to determine the chemical composition of larger features. Bright-field transmission electron microscope (TEM) images, Fast Fourier Transform (FFT) and EDS spectra of smaller features were acquired with a JEOL 2010F TEM.

2.2.5. Sheet Resistance

The resistance of a transparent electrode is a critical factor that acquires precise control during the electrode fabrication process depending on the desired application. For example, in modern display and touchscreen applications, in order to allow for fast screen response, the sheet resistance of the transparent electrode has to be below 10 $\Omega/\square$. If the sheet resistance was higher, the entire device display would not respond immediately- instead there would be a delay in pixel response. On the other hand, some applications such as capacitive touchscreens do not require an ultra-low sheet resistance to perform efficiently- but generally the speed of the device using the transparent electrode material is dictated by their sheet resistance values [98].

Resistance of a material is related to resistivity through:

$$R = \rho \frac{L}{Wt}$$

where ρ is the resistivity of the sample (units of Ω•cm), L is the length of the sample, W is the width of the sample, and t is the thickness of the sample. The resistance of transparent electrodes is instead most often characterized by sheet resistance, R_s:

$$R_s = \frac{\rho}{t} \ [\Omega/\square]$$

$$R = R_s \frac{L}{W}$$

where the sheet resistance has units of $\Omega/\square$. Sheet resistance is particularly useful for NW electrodes which do not make a continuous film and thus the film thickness is hard to define. Sheet resistance is mostly used for better comparison between performance metrics of transparent electrodes of different types/materials.

2.2.6. Transparency

Transparency is the ability of light to pass through an object. In regards to visible light, transparency can change depending on the wavelength of light passing through the object (red light may not pass through the object as easily as violet light). Furthermore, when light encounters an object, it can be transmitted, absorbed, or reflected depending on the object material properties. The ratio of the transmitted light through the object to the incident light radiated from the source is referred to as the transmittance.

In regards to the present work, transparencies will always be reported as a percentage of incident light reflected at a specified wavelength of 550 nm (peak wavelength of sunlight is 550 nm) [99]. Furthermore, all transparencies will be in reference to the substrate (i.e. the transmittance of the glass, plastic, or stated substrates will not be included in the transmittance value) unless stated otherwise.

When observing the full range of light transmitted, one has to account for light scattered by the interaction object- often referred to haze. Haze is a phenomenon experienced when

incident light is scattered while being transmitted through the interaction object, and is detected

off-axis from the majority of the transmitted light. Substrates such as glass or plastic and

transparent conducting oxides such as ITO do not scatter a significant amount of light. However,

silver nanowires do scatter a portion of incident light (which is heavily dependent on the amount

of nanowires in the network, as dense networks scatter a significant amount of light). In order to

comply with standards related to a variety of applications such as display technologies,

transparent electrodes must not scatter more than 3% of incident light (or scatter the light by an

angle more than 2.5° from the original source) [100].

2.2.7. *Electrical Conductivity Stability Testing*

In order to reliably test the conductivity of the AgNWs over an extended period of time,

conductive contacts were required to be placed on the nanowire film. Strips of copper tape were

placed on the ends of every fabricated electrode in order to allow for ease of measurement using

a digital multimeter (discussed below).

2.2.8. *Determining nanowire film density*

As will be discussed in detail in in Chapter 3, the density of the NWs in an electrode

affects the rate of electrode degradation. Most papers in the literature do not state the density of

NWs used, so calculations were required to determine the density of NWs used from the images

provided in their papers. For silver nanowire density calculations, Image J software is used for

easy comparison of previous work performed in literature. Images from papers were imported

into ImageJ and subjected to image processing by the software. Image contrasts were modified

until there were exclusively black and white pixels (white pixels were nanowires, black pixels

were substrate). The number of white pixels was divided against the total number of white and

black pixels to determine the surface coverage of the AgNWs. Surface area and volumes of the

AgNWs were then calculated using measured diameters in the image processing software. Once the volume of AgNWs was calculated, it was converted to a mass via the density of silver. The mass of silver was then divided by the total area of the picture, determined using ImageJ, and the scalebars of the images) to determine the network density in g/cm^2.

2.2.9. *Electrode Storage Conditions:*

All fabricated electrodes were stored in an atmospherically regulated environment (average temperature: 24±1°C, humidity 40±2%) with ambient airflow for 60 days. Humidity and temperature were tracked using an InkBird ITH-10 Hygrometer. The electrodes were stored in the dark to avoid any photonic influences on nanowire behaviour throughout the test. Electrodes were periodically removed for several seconds every 3 days throughout the study for sheet resistance measurements. Furthermore, electrodes fabricated using the same solution parameters were stored in a dark low-vacuum environment to observe if there were any changes in sheet resistance in an environment almost devoid of ambient gases.

Chapter 3:   The Dependence of Silver Nanowire Stability on Network Composition and Processing Parameters

Several topics related to the passive stability of silver nanowires are presented in this chapter. Specifically, the major artifacts of corrosion in AgNW films, the composition of corroded AgNW films, parameters affecting the stability of AgNW films, and suggestions to minimize the rates of degradation in nanowire films are presented. This chapter is reproduced from our recent published manuscript in RSC Advances 2017 [101].

3.1. Introduction

AgNWs have very high surface area to volume ratios due to their shape and small diameter (< 100 nm). Due to these physical characteristics, instability and corrosion can be severe problems. AgNWs have been known to become discontinuous when left in atmospheric conditions for less than 6 months [64] that leads to electrode failure. Because of the surging interest in the use of AgNW as a replacement for ITO, the longevity of the material and the causes of their degradation must be understood before AgNW electrodes can be more widely used in commercial applications.

As stated in Chapter 1, there is very little knowledge about the stability of AgNWs when exposed to atmospheric conditions. Studies that focus on AgNW stability state their reactions to factors such as humidity [65], high temperatures [66], light [65], and high electrical currents [63], which are proven to accelerate the degradation of AgNWs. Furthermore (as previously stated in 1.4.2.), the rates of degradations differ significantly between all studies referenced.

The motivation for this chapter is based on the differences between passive AgNW corrosion studies. There is very little consensus between the studies performed by Mayousse [67], Elechiguerra [64], Moon [69], and Vaagensmith [74] despite their similar experimental

conditions. Further investigation into the lifetime of AgNWs is necessary, as a proper understanding of the corrosion rates of AgNWs when exposed to a variety of conditions would be useful for future researchers developing devices where AgNW integration is necessary.

In this chapter we study how the electrode composition and common processing parameters used to fabricate these electrodes affect nanowire stability and electrode lifetimes. AgNW electrode films were prepared using a variety of different solvents, substrates, nanowire diameters, film densities, and various pre- and post- treatment processing parameters, then exposed to atmospheric conditions for an extended period of time. The results observed reveal valuable information on what variables affect silver nanowire degradation and therefore how to increase the lifetime of silver nanowire materials. Specifically, it was observed that the nanowire diameter, density, post-deposition annealing temperatures and substrate plasma treatments are parameters that significantly affect the longevity of AgNW electrodes.

3.2. Experimental Details

Silver nanowires dispersed in ethanol were purchased from Novarials Inc. (Woburn, Massachusetts), with average diameters of 20 nm and 70 nm and average lengths of 20 μm and 50 μm respectively, and nanowires dispersed in isopropyl alcohol were purchased from Blue Nano Inc. (Charlotte, North Carolina), with an average diameter of 90 nm and length of 40 μm. AgNWs were also purchased from ACS materials (Pasadena, California) at diameters of 30 nm and 50 nm , with lengths of 100-200 μm. The AgNWs were then deposited as random networks onto glass, silicon and PET substrates. AgNW electrodes were fabricated via the Mayer rod method as described in Chapter 2.

3.3. Results and Discussion

3.3.1. Parameters Not Affecting Degradation Rates

Not all processing variations and physical characteristics of the AgNWs tested affected how quickly network degradation occurred, and these variables are covered in this section. Firstly, it was suspected that the material used for solvent storage might have an effect on the degradation rates of AgNW networks, because the polyvinyl pyrrolidone (PVP) that remains on the surface of an AgNW after synthesis readily dissolves in polar solvents such as water and ethanol [27]. Thus, storage in these solvents may affect the thickness or presence of PVP on the AgNWs in solution, and it has been postulated by Elechiguerra [64] that PVP may play a role in slowing AgNW corrosion. Furthermore, manufacturers of AgNWs store and ship the material in a variety of solvents, mostly water, ethanol, or isopropyl alcohol (IPA), and thus it is important to know if these solvents will have any effect on the degradation rates of AgNWs. To test the effect of the type of solvent, 20 nm diameter AgNWs were purchased from Novarials dispersed in both in ethanol and IPA, and similar diameter AgNWs dispersed in water were acquired from Seashell (California). Nanowire electrodes were fabricated according to the procedure listed in chapter 2 of this document. The fabricated electrodes were then left to age in dark ambient conditions, and had sheet resistances measured for a total of 60 days. After 60 days, there was no significant difference in sheet resistance increase between the fabricated samples. It is speculated that the type of solvent used for storage of the AgNWs had no significant effect on their corrosion rate because the solvents could not dissolve the PVP on the AgNWs.

Also related to storage conditions is the amount of time the NWs were stored in solution before being deposited as a film. Manufacturers of AgNWs suggest that the material expires after approximately 1 year from date of AgNW synthesis, suggesting that electrode performance

may not be similar after sitting for an extended period of time. Perhaps the nanowires could degrade to nano-rods of only a few μm in length (to be discussed in the following sections). To test this, 90 nm AgNWs from Blue Nano were purchased and electrodes were fabricated immediately, while electrodes were also made using the same nanowires purchased 3 years prior which had been sitting in in solution for all that time. Immediately after fabrication, both electrodes exhibited similar sheet resistances and transparencies (14.1 $\Omega/\square$ for the aged AgNWs at 88%, 13.7 $\Omega/\square$ at 88% for the new AgNWs). After 60 days, it was observed that there was less than 10% difference between sheet resistances after corrosion occurred. Both nanowire samples had sheet resistance increases at similar rates with no significant deviations. From this study, it is observed that the age of the nanowires in solution does not have any significant effect on the corrosion resistance or electrode performance.

The length of the fabricated AgNWs was also suspected to have some effect on AgNW corrosion rates. It was postulated that a longer nanowire) would have a stabilizing effect on the electrode by preventing Ag diffusion across the sample (to be discussed later) [102] [103]. 100 μm long AgNWs with diameters of 30 nm were purchased from ACS Materials, and AgNWs with the same average diameter of 30 nm but an average length of 6 μm were purchased from a local supplier. Electrodes using the same AgNW solution concentration (i.e. 4 mg/mL) were fabricated and left to age for 60 days in ambient. After 60 days, it was observed that there was no significant difference in the rate of sheet resistance increase between the two electrodes. The extra length of the AgNW had no significant effect on corrosion resistance.

AgNWs have been used on various substrates by many researchers recently [42, 47, 35, 33, 37]. Because of the versatility of AgNWs as a material, researchers have used them in both applications that require flexible substrates such as polyethylene terephthalate (PET), and rigid

substrates such as glass. However, the surface energies of these substrates differ, which will affect the adhesion of the AgNWs to the substrate. More importantly, the differences in their surface energy could allow for a more hydrophilic substrate surface, leading to increased moisture which is known to increase corrosion rates of AgNWs [104]. This increased surface energy has a significant effect on the contact angle of the surface as a whole- allowing an ease of binding for any free moisture in the atmosphere to the substrate surface- increasing the likelihood of the formation of monolayers of surface water (even in a dry testing environment) [105]. For these reasons, it was suggested that the use of both glass and PET substrates (the two most reported substrates in literature) be used as substrates for AgNW electrode fabrication to observe if there was any significant difference in corrosion rate between them. AgNW electrodes were fabricated on both glass and PET substrates using Novarials A20 nanowires. After 60 days in ambient, there were no significant differences in sheet resistance increase (both increased at similar rates, with a 13% difference in final sheet resistance increase between the glass and PET samples). This result is not significant and thus the conclusion has been made that there is little difference in corrosion rate amongst common substrates used in AgNW electrode fabrication.

3.3.2. *Parameters Affecting Degradation Rates*

Out of all variables tested, four parameters had a significant effect on the resistance change of the nanowire network over time: nanowire diameter, nanowire concentration, annealing temperature, and substrate plasma treatment. Figure 3-1 shows the effect of these variables on electrode sheet resistance over a period of 60 days of ambient atmospheric exposure. The effect of each of these variables on the NW network will be discussed in detail in the sections below, but first we will compile the main degradation artifacts that were observed since they are common to several parameters.

For the remainder of this communication, percentage changes in sheet resistance will be performed using the formula in equation 1:

$$\Delta R_S = \frac{R_S - R_O}{R_O} \times 100\% \qquad\qquad (1)$$

Where ΔR_s is the percentage change in sheet resistance, R_S is the measured sheet resistance value, and R_O is the sheet resistance recorded at the time of fabrication (day 0).
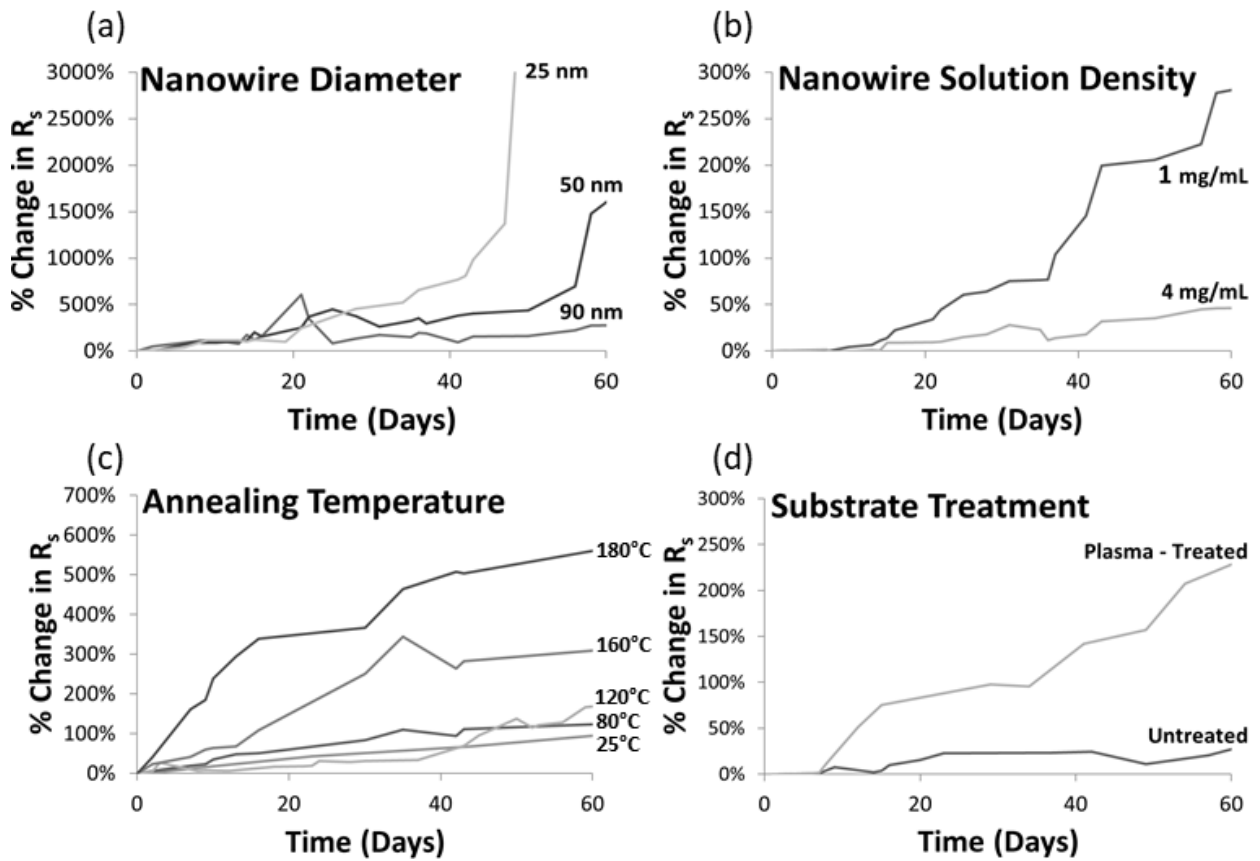
Figure 3-1: The effect of electrode and processing parameters on electrode sheet resistance (Rs) when left in air for 60 days. (a) Nanowire diameter, (b) nanowire density, (c) annealing temperature, (d) substrate plasma treatment sheet resistances were calculated using equation 1.

3.3.3. Degradation Artifacts

After 60 days in atmosphere, silver nanowires degrade and become discontinuous in more than one manner. Figure 3-2 shows the morphology and chemical composition of the three

main degradation artifacts that were observed. First, shown in Figure 3-2a, is the formation of many small nanoparticles along the surface of a nanowire. TEM-EDS spectra of these nanoparticles (Figure 3-2d) show that other than carbon originating from the TEM grid and silicon signal from the detector, only silver and sulfur are present. From studies on bulk silver it is well known that silver does not form a native oxide in atmospheric conditions, but rather silver sulfide (Ag_2S) is the dominant product of corrosion [106, 104, 107, 108, 109].The latter occurs via the reaction of surface silver with atmospheric hydrogen sulfide (H_2S) and carbonyl sulfide (OCS), even though these have very low ambient concentrations of 5 ppb and 0.5 ppb, respectively [104]. Ag_2S nucleates at random locations on the surface of silver and tends not form a uniform film [40]. Rather, morphologies including dendrites, clumps and whiskers have been observed on bulk and thin films of silver. For AgNWs, several reports observe that Ag_2S exists as particles along the surface of the nanowire body [110, 65, 63, 67]. After the 60 day experiment, some silver nanowires corrode to the point of discontinuity, as displayed in Figure 3-2a. The time lapse of corrosion can be observed in Figure 3-3, with separation between nanowire halves occurring between week 2 and week 4 of the nanowire being exposed to ambient conditions- with the bulk of the Ag_2S formation occurring after week 4 of being exposed to ambient.
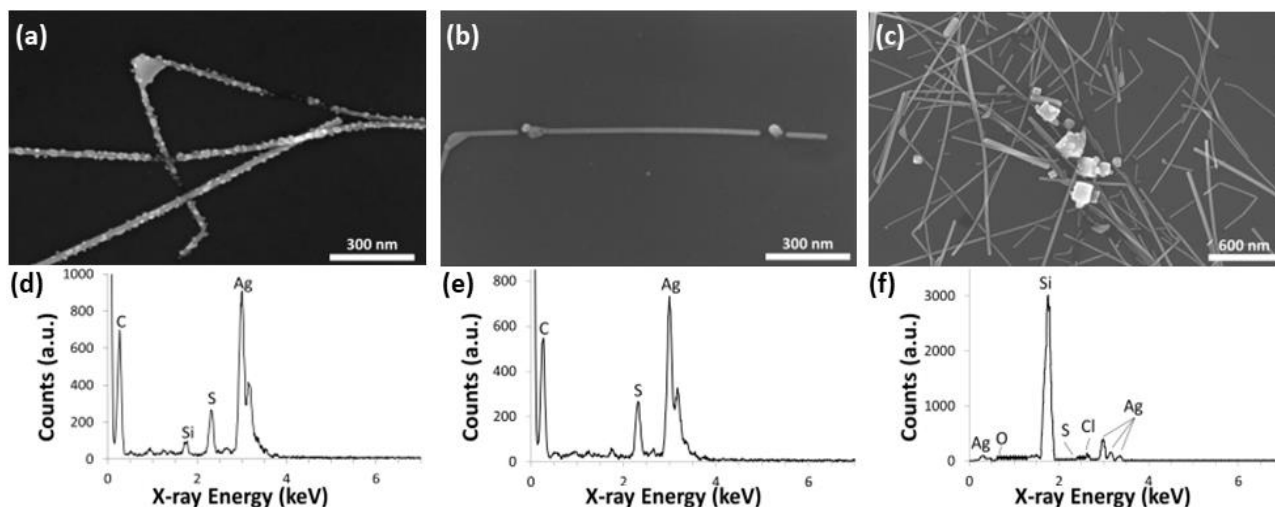
Figure 3-2: SEM images of silver nanowires exposed to atmosphere for 60 days. There are 3 main types of degradation artifacts observed: (a) small Ag2S particles on the surface nanowires, (b) spherical silver particles intercepting a nanowire, and (c) clusters of larger agglomerations of silver. (d) TEM-EDS spectrum of one nanoparticle on the surface of a nanowire in 'a', (e) TEM-EDS spectrum one particle intercepting the nanowire in 'b', and (f) SEM-EDS of a larger particle in 'c' (the silicon peak originates from the substrate).
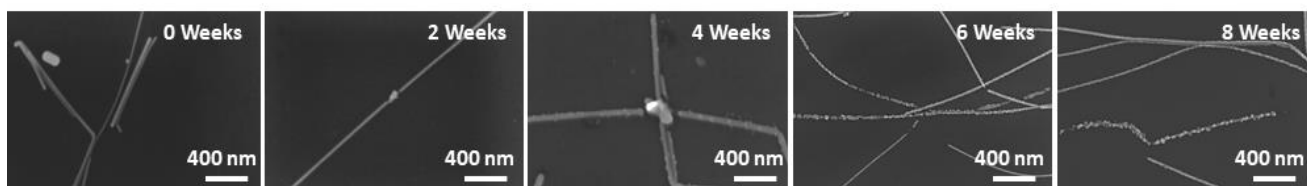
Figure 3-3: Time lapse of AgNWs exposed to ambient conditions showing the formation of Ag_2S particles from corrosion caused by H_2S

Corrosion of AgNWs was present under all experimental parameters tested in this work, but was not always the dominant failure mechanism causing discontinuity in the nanowire network. Spherical particles intercepting the nanowire body were observed as a second artifact causing discontinuity of nanowires over the 60 days (Figure 3-2b). This artifact was observed in thinner diameter nanowires either in sparser networks or ones isolated from the main AgNW network. Nanowires with these intercepting particles do not have small Ag_2S nanoparticles on their surfaces. High-resolution TEM shows that the intercepting particles are polycrystalline, and EDS analysis of several of the particles indicates that they are predominantly silver (85-91%), with 1-2% chlorine and 7-13% sulfur. Regarding the chlorine, this atomic percentage is slightly higher than in areas of the nanowire away from the particles (< 1%). AgCl can be a result of Ag

34

reacting with trace amounts of Cl_2 and HCl in the ambient [106, 104]. The chlorine could also be

left over from the synthesis process as NaCl is commonly used in the polyol synthesis method.

Regardless, the majority of the particles are Ag suggesting that they do not primarily exist of

corrosion products, but are rather a result of a rearrangement of silver from the nanowire into

nanoparticle form due to the morphological instability of the nanowire. These issues will be

discussed in the sections below. Figure 3-3 shows the time-lapse formation of these small

particles in a nanowire network with discontinuity of the nanowire caused by these spherical

particles being observed during the week 4 SEM image, indicating the nanowire network became

discontinuous between week 2 and week 4 of the study. Furthermore, Fast Fourier Transform

(FFT) analysis of a spherical particle is available in Figure 3-5 and Figure 3-6 as a comparison to

the crystal structure of a fresh AgNW). The diffuse rings in the FFT analysis indicate some

polycrystalline material, but the spot patterns typical of pure Ag are still evident on spots 1

through 6. (The highlighted area in Figure 3-5 was analyzed due to stacking faults present in the

darker regions of the TEM image). This corroborates with the EDS data showing that the

particles are predominately silver.
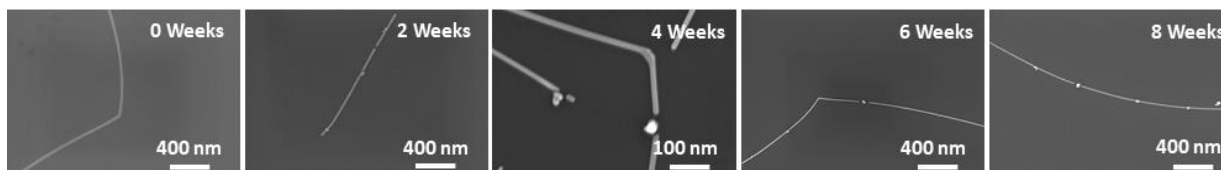
Figure 3-4: Time lapse of AgNWs exposed to ambient conditions showing the formation of spherical particles eventually bisecting the AgNW- causing discontinuity in the network
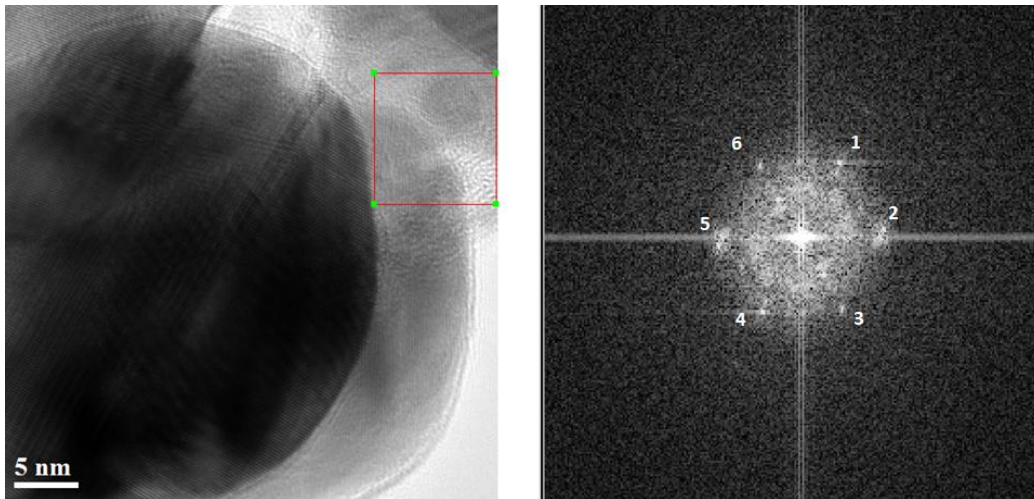
Figure 3-5: FFT analysis of a spherical particle bisecting a small diameter AgNW. The selected region was analyzed to avoid overlapping from stacking faults present throughout the particle
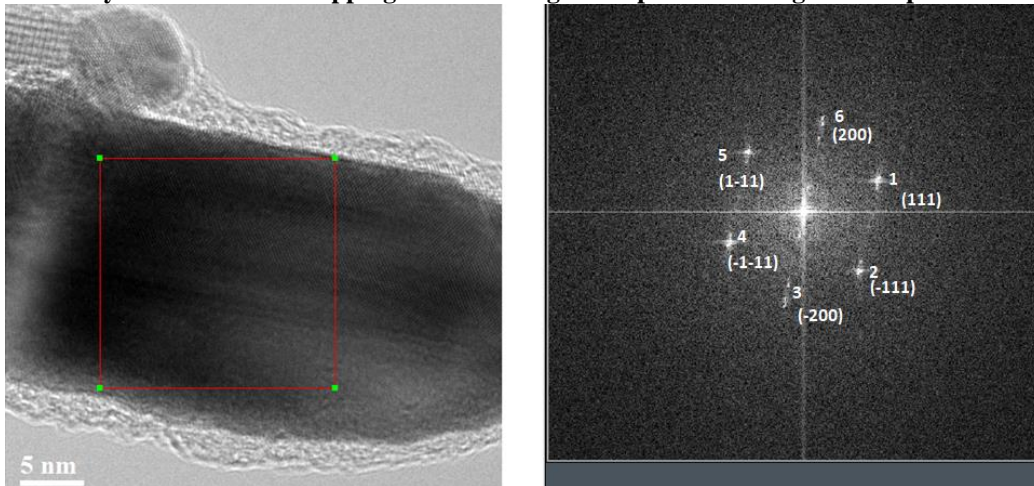
Figure 3-6: FFT analysis of an un-aged AgNW body to show the crystal facets of an unperturbed AgNW

The last major artifact observed was clusters of larger agglomerations that were prevalent in dense networks of thinner nanowires. From the SEM image in Figure 3-2c, one can see that there is no presence of either Ag_2S nanoparticle growth or intercepting spherical particles in any of the nanowires in the vicinity of the agglomerations. SEM-EDS results show that the large agglomerations consisted primarily of Ag (90-94%) with some amount of Cl (6-10 %) and trace sulfur (silicon is present in the EDS spectrum due to its use as a substrate material). Thus, the large particles are mostly silver that has likely diffused from the AgNWs in the network [107, 108]. This will be discussed further below. The diffusion of silver atoms causes discontinuities in nanowires in the network, as can be seen in Figure 3-2c.

36

In the subsections below, the effect of the significant variables - diameter, density, annealing temperature, and plasma treatment - are discussed in more detail.

3.3.4. Effect of Diameter on Degradation Rate

There can be a degree of control imparted over the synthesis of AgNWs in which researchers are able to control the diameter and length of the AgNWs through the variance of certain synthesis parameters (such as the addition of more NaCl or KBr to the reaction vessel) [111]. Furthermore, filtration methods of AgNWs are now accurate enough to allow for the processing of diameters to within a range of +/- 10 nm [112]. This allows industrial manufacturers the ability of offering a wide range of diameters and thus NW diameter is one design choice an engineer has when developing an electrode. Therefore, knowing if and how the diameter of AgNWs affects corrosion rates is important information. In order to test this hypothesis, AgNWs were purchased with diameters of 20 nm, 50 nm, and 90 nm, and placed in ambient conditions after formation of transparent electrodes as stated in chapter 2 of this thesis.

Figure 3-1a plots the percentage change in resistance of electrodes prepared with different diameter nanowires deposited with the same nanowire solution concentration of 4 mg/mL. The plot shows that electrodes consisting of thinner nanowires degraded significantly faster than those with thicker nanowires. After 60 days, the sheet resistance of electrodes with 90 nm and 50 nm diameter nanowires increased 250% and 1600%, respectively. Electrodes with 25 nm diameter nanowires reached an open-circuit before the 60 days was over.
The degradation of larger diameter nanowires (greater than 40 nm in diameter) is primarily caused by corrosion creating Ag_2S nanoparticles on their surface, as shown in Figure 3-1a, Figure 3-2, and again in Figure 3-7a. The thicker the nanowire, the longer it takes for corrosion to advance to the point where the nanowire becomes discontinuous. Therefore, electrodes made

from thicker nanowires have longer lifetimes. In order to confirm that Ag_2S formation was occurring on the surface of thicker nanowires, TEM images and corresponding Fast Fourier Transform (FFT) images of the corroded large diameter nanowires were observed. Analysis of the d-spacing on the spot pattern states that the majority of the spots on the FFT correspond with Ag_2S to a percent difference below 5%. There is very little to no matching of spot patterns to either pure silver or AgCl (the latter being another possible corrosion product of silver).
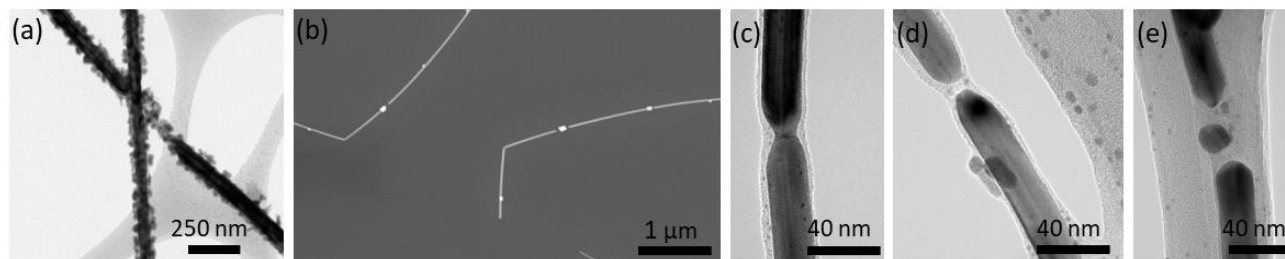
Figure 3-7: Images of silver nanowires left in atmosphere for 60 days. (a) TEM image of larger diameter (90 nm) nanowires indicating corrosion. (b) SEM image of smaller diameter (20 nm) nanowires showing particles at the location of disconnects in the nanowires. TEM images showing the progression of particle formation in small diameter nanowires over time: (c) beginning of bottleneck formation, (d) a bottleneck that has progressed into discontinuity, (e) a spherical particle and a wider nanowire disconnection

In smaller diameter nanowires (diameters less than 40 nm), degradation by the corrosion depicted in Figure 3-1a was scarcely observed. Rather, as seen in Figure 3-11b, the prevalent degradation matches the artifact depicted in Figure 3-1b. Figure 3-11c - e displays TEM images of smaller diameter nanowires at different stages of degradation, from bottlenecking (Figure 3-11c), to disconnection (Figure 3-11d), to particle formation (Figure 3-11e). The morphological changes in the nanowire, coupled with the EDS data showing that the main composition of the spherical particles is silver rather than corrosion products (Figure 3-1e), indicate that nanowire instability rather than corrosion is the primary reason for thin nanowire degradation. The surface-area-to-volume ratio of nanowires scales with 1/r, where r is the radius of the nanowire. Thus this ratio is more than 3.5 times higher for a cylindrical 25 nm diameter nanowire versus a 90 nm nanowire (Table 3-1). And because surfaces have higher energy than atoms in bulk, thinner

nanowires are less stable than thicker ones. This is particularly true for Ag nanowires whose side facets are {100} [109], which for face-centre-cubic materials have higher energy than the lowest energy {111} facets. Furthermore, silver nanowires synthesized from the polyol process have strain energy caused by a combined 7.35° gap between the triangular prisms forming the pentagonal wire [102]. The observation of thin metal nanowires breaking into smaller segments has been observed and studied by others and is often attributed to Raleigh instability [113, 114, 115, 116, 103, 117]. Bottlenecking, as observed in Figure 3-1c, likely starts at a location of high energy such as at the edge of two intersecting {100} facets.

SEM data show that the instability of thin nanowires in air causes a larger proportion of them being discontinuous after 60 days compared to thicker diameter nanowires. The latter are more stable due to their lower surface area per volume and instead degrade due to corrosion, which leads to discontinuities at a much slower rate. These observations explain the more rapid resistance increase of the electrodes containing 25 nm diameter nanowires in Figure 3-1a compared to electrodes with 50 and 90 nm diameter nanowires.

Table 3-1: Surface area-to-volume ratio of nanowires used in the study. Nanowire lengths have been equated to show effect on SA/V ratio

Nanowire diameter (nm)	Average Length (nm)	Average Surface area (nm^2)	Average Volume (nm^3)	Average SA/V
20±5	35000	2.20E+06	1.10E+07	0.200±0.050
35±8	35000	3.85E+06	3.37E+07	0.114±0.029
50±10	35000	5.50E+06	6.87E+07	0.080±0.020
70±10	35000	7.70E+06	1.35E+08	0.057±0.014
90±20	35000	9.91E+06	2.23E+08	0.045±0.011

Table 3-1 states the advertised surface area to volume ratio used in this study. It is important to note that during polyol synthesis, not all nanowires will grow to be the same length or diameter. The growth conditions of the bath will give rise to AgNWs with a variety of diameters and lengths, which models a Gaussian profile. The Gaussian profile has a midpoint of the diameters /lengths listed in Table 3-1, with a 3 standard deviation profile stating the larger/smaller diameter of the key measurements of the nanowire. Therefore, Table 3-1 states the average length and diameter of nanowires purchased from a variety of vendors. Based on information received from the vendors, the diameters of the nanowires are as follows: 20 ±5 nm, 35 ±8 nm, 50 ±10 nm, 70± 10 nm, and 90 ±20 nm. One could also speculate that the lengths of the AgNWs supplied varies significantly (assumed to be by ~20%, as no distribution of lengths was supplied by the vendors due to researchers only desiring accurate diameter measurements- and SEM images did not show a full nanowire in most cases). Based on this information, one could speculate that the SA/V ratio in Table 3-1 could vary by approximately 25%.

Furthermore, measurements using SEM were performed to measure the length and diameter of AgNWs deposited onto substrates. Although there were approximately 50 measurements taken of different nanowires, this sample only represents a 1µm x 1µm area of the total 4cm x 4cm substrate (or 1×10^{-6}% of the overall sample).

The key observation of this study states that larger diameter AgNWs are inherently more stable than smaller diameter AgNWs because of their reduced surface-to-volume ratio, allowing for a lower total surface energy than their smaller diameter counterparts. Larger diameter AgNWs undergo the growth of Ag_2S as their primary method of degradation, as confirmed by SEM, TEM, EDS, and FFT as their primary methods of corrosion. Smaller diameters AgNWs undergo degradation in the form of Rayleigh instabilities and some formation of Ag_2S at their

surface. Furthermore, it is observed that smaller diameter AgNWs degrade at a much faster rate than large diameter AgNWs, as electrodes fabricated with 20 nm AgNWs became discontinuous to the point of non-conductivity before the 60 day study concluded, while electrodes fabricated from 90 nm AgNWs had the lowest overall increase in sheet resistance after the 60 day study.

This study has some very key implications for designers of display technologies, as the size of the AgNW can affect its end application. Because AgNWs of large diameters have a greater effect on light scattering than smaller diameter AgNWs, they can only be used in certain applications below specific concentrations [118]. As an example, the display market requires scattered light in the form of haze to be below 2% in order for a light emission device to be considered an acceptable quality for use [118]. This application will likely require the use of very thin diameter AgNWs in order to meet quality demands for industrial and consumer use. Meanwhile, applications such as solar panels require a high degree of scattered light to prevent total internal reflection- allowing for the absorption of more light and production of energy [118]. In this case, the high haze imparted by the large diameter AgNWs will be well suited to the application. Regardless of the end application, future transparent electrode design will need to factor in the varying degradation rates of different diameter NWs. A potentially even more useful outcome of this study is that we now know that small and large diameter NWs degrade through different mechanisms and thus methods to improve lifetimes may be different depending on the diameter used. For example, since smaller diameter NWs have a morphological instability problem, strategies to increase their morphological stability may be helpful such as low temperature hydrogen gas processing [119] or passivating the silver surfaces with dielectric layers [120, 121].

3.3.5. Effects of Density

The density of an AgNW network affects many of its electrical and transparent parameters. Denser AgNW networks provide a higher degree of overlapping and junctions in-between individual AgNWs, providing more conductive pathways for electrical signals to travel through (resulting in a low sheet resistance i.e. < 10 $\Omega/\square$). However, denser networks of AgNWs cover more of the substrate surface, resulting in a lower transparency and higher degree of scattered light. There exists a trade-off between sheet resistance and transparency that will need to be addressed by the designer of the AgNW final application. The information available in this study could also affect future transparent electrode design, as there may be a minimum or maximum NW concentration for the longest-lifetime. In order to observe the effects of density on corrosion of a AgNW network, concentrated solutions of AgNWs (4 mg/mL) and low concentration solutions of AgNWs (0.2 mg/mL) were used to fabricate electrode samples. These samples were left to age in the environment as described in chapter 2 of this text, with periodic observance of the sheet resistance and imaging using SEM.

As seen in Figure 3-1b, the sheet resistance of dense nanowire networks (made with a solution concentration of 4 mg/mL) increased only 50%, while a sparse network (solution concentration = 0.2 mg/mL) containing nanowires of the same diameter and prepared in the same manner, increased by over 300%.

The varying density electrodes fabricated in this series of experiments were prepared with 20 nm diameter nanowires. Since the diameter was small, little evidence of the type of corrosion depicted in Figure 3-1a is observed, as discussed in the section above. However, microscopy imaging did reveal the degradation features in the dense and sparse networks differed. In sparse networks (solution concentration ≤ 0.5 mg/mL), the formation of small particles as described in

Figure 3-1b is dominant. However, in dense networks (solution concentration ≥ 4 mg/mL) the

dominant degradation feature is instead the one depicted in Figure 3-1c. These large particles

appear to be the primary degradation artifact in dense samples (Figure 3-13). Originally it was

thought that the large particulate formations in the latter were artifacts of AgNW synthesis that

penetrated the filtration mechanisms used for nanowire purification, but SEM of freshly

synthesized networks had no evidence of such large particles. Only after exposure to ambient

conditions for approximately 4 weeks were these features first observed- indicating that these

large particles are artifacts of degradation in the dense AgNW network.
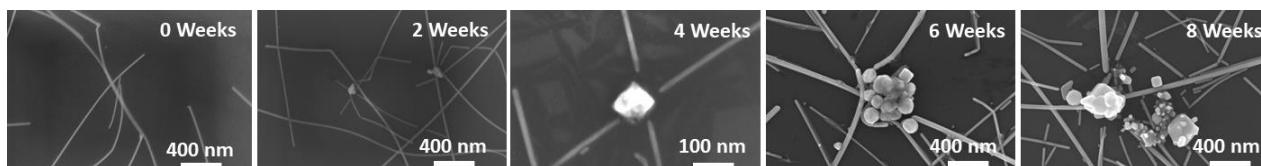
Figure 3-8: Time lapse of AgNWs exposed to ambient conditions showing the formation large particles. The particles on average become larger over time. It is suspected that these large particles are formed from diffusing silver from the AgNW network.

Although the appearance of degradation differed among sparse and dense networks, it

was found from extensive SEM imaging that the proportion of nanowires with an electrical

discontinuity was the same regardless of density (Figure 3-4 and Figure 3-8). Through all of the

SEM analysis performed, AgNWs all appeared to show artifacts of corrosion after similar time

periods regardless of the network density. In regards to the spacing between discontinuities in the

AgNW network, there was one discontinuity per 1 μm length of nanowire on average after 60

days of exposure to ambient conditions. Thus, a denser network did not increase nanowire

stability. Rather, the dense network has a slower increase in resistance because if a nanowire

becomes discontinuous, there exists other pathways through which the current can flow. Sparser

networks, on the other hand, have fewer alternative conductive pathways when an electrical

disconnection occurs- meaning the sheet resistance of these samples would increase rapidly for

every conductive pathway that became severed due to degradation. This explains the behaviour

of the curves in Figure 3-10b- as the sparser AgNW electrode sample had a much higher sheet resistance increase than the denser sample due to the discontinuity appearing in the conductive pathways of the electrode. EDS analysis of such features (Figure 3-2f) indicates that these agglomerations are composed primarily of elemental Ag (Table 3-2), like the small particles encountered in sparse networks. The volume of silver in these particles is larger than amount of the silver missing from the nanowires in their immediate vicinity. It appears that much of the Ag in the particles have diffused from nanowires further away, as evidenced by gaps in nanowires up to 1.5 μm away from the agglomerations. The gaps do not have small particles intercepting them and it is hypothesized this is because the small particles that result from nanowire instability, or the silver that would otherwise lead to them, diffuse and coalesce to form the larger agglomerations similar to an Oswald ripening process. Because the surface-to-volume ratio of particles decreases with their size, a large particle is more energetically favourable than multiple smaller particles. Larger particles are not observed in sparser networks likely because the small particles are far apart and they would need to diffuse markedly longer distances to coalesce.

Table 3-2: Breakdown of elemental percentages in large particle growth (from EDS data in Figure 3-1f). Oxygen was omitted from the calculation because of the silicon oxide present on the substrate used for imaging

Element	Element wt%	Element Atomic %
S	0.36	0.98
Cl	7.37	18.14
Ag	92.27	80.88

A breakdown of the elements present in an EDS spectrum (taken from large particles such as those available in Figure 3-2c) is shown in Table 3-2. The low concentrations of Ag_2S and AgCl in these large growths indicate that the structure is composed primarily of elemental Ag. However, the high concentration of Cl in the EDS spectrum indicates that there may be Cl contamination from ambient or Cl in the AgNWs. The presence of Cl_2 in the atmosphere is very

low, but can cause some degree of corrosion in the AgNW network according to Franey and Graedel [122, 104]. As mentioned in section, it is possible that Cl is leftover from synthesis, as NaCl is used to help the dissociation of silver nitrate in the polyol process- and to aid in the seeding process of synthesis [123]. NaCl is also useful for physical dimension control, as increased levels of chlorine in synthesis allow for much thinner AgNWs [124]. Because AgNWs from Novarials were stored in ethanol and IPA (of which NaCl is insoluble in both of these solvents), leftover NaCl from synthesis is likely not possible as it would be removed from the complete AgNW solution from the filtration process. A possible explanation for the high concentration of Cl in these large agglomerations could be due to trapped Cl ions in the AgNWs during synthesis. It is suspected that the dissociation of NaCl into Na^+ and Cl^- would cause some chlorine ion to form ionic bonds with the Ag^+ used to form a nanowire. As previously discussed, a higher concentration of NaCl during AgNW synthesis allows for the formation of smaller diameter AgNWs. This high concentration of Cl^- used during synthesis would have a significant impact on the Novarials A20 AgNWs. . Furthermore, Ag^+ ions would diffuse towards a negatively charged source such as a Cl^- ion present in the AgNW electrode- leading one to believe that the Cl in these large particles is the primary factor in their growth.

Based on the information available in the above study, one can determine that a denser AgNW network will offer a longer lifetime than a sparser AgNW network. Once again though, there are trade-offs between electrode density, transparency and electrical performance of the electrode. The denser AgNW networks may offer a longer lifetime and higher performance in terms of low sheet resistance, but there will be less light transmission as well as more haze [5]. These latter factors in tandem with lifetime considerations need to be taken into account.

3.3.6. Effect of Annealing Temperature

When AgNW films are deposited on a substrate without further processing, locations where nanowires overlap have a high resistance that can lead to film sheet resistances in the MΩ/□ range. Annealing significantly lowers junction resistances and therefore film sheet resistance by welding the overlapping nanowires, and is the most commonly used and convenient method to do so. The most common annealing condition for lowering the sheet resistance in AgNW electrodes is 200 °C for 30 minutes [89, 30, 6, 95]. Thermal treatments such as annealing are often performed on metallic nanowire networks as a strategy to significantly lower the network's sheet resistance. Welding at the nanowire junction occurs in metallic nanowire networks at an elevated temperature, allowing for a much stronger current to be carried through the network [113]. The PVP coating on the AgNWs is an artifact of their synthesis creating a non-conductive sheath preventing full Ag-Ag contact at nanowire junctions [123], and as a result needs to be heated to above 150°C in order to remove PVP from the nanowire surface through the polymer's dissociation above that temperature [125]. As a result, thermal annealing has become a popular treatment technique for AgNWs in both industry and research alike.

The effect of the annealing temperature on electrode lifetimes, however, has not previously been studied. Perhaps the thermal treatment applied to remove PVP from the AgNW body allows for faster diffusion of H_2S to the surface of the AgNW. This faster diffusion of H_2S caused by a thinner PVP layer (or non-existent PVP layer) could result in an accelerated corrosion rate. Furthermore, corrosion rates are increased at higher temperatures according to Franey [104] which may also affect the lifetime of AgNWs under annealing conditions. Another possibility is that the PVP allows for easier formation of water monolayers on the surface of the AgNW since it is hydrophillic (due to the outwards orientation of the CH_2 polymer chain of the

PVP), resulting in easier adsorption of H_2S. Blue Nano 90 nm nanowire samples were annealed at various temperatures listed in Table 3-4 and aged for 60 days alongside a nanowire sample that was pressed at room temperature. SEM images were taken and sheet resistances were observed over the 60 day period to allow for quantification of any detrimental effects occurring to the nanowire network.

Although a 30 minute anneal significantly reduces the initial sheet resistance, it accelerates the rate of degradation over the long term. Figure 3-1c, where 25 nm diameter AgNWs are annealed at different temperatures, reveals that the higher the annealing temperature used, the faster the electrode resistance increases over time. The sheet resistance of electrodes annealed at 180 °C for 30 mins increased 590% over the 60 day time period compared to 137% for samples annealed at 80 °C. The resistance of electrodes that were mechanically pressed at room temperature rather than annealed rose 97% (Table 3-3).

Table 3-3: Change in sheet resistance after 60 days after annealing at elevated temperatures for 30 minutes during electrode processing.

Annealing Temperature	$\dfrac{\Delta R}{R_o} - 100\%$
25°C	97%
80°C	137%
120°C	172%
160°C	320%
180°C	590%

Two samples of 90 nm diameter nanowires, one annealed at 150 °C for 30 mins and one pressed at room temperature after nanowire film deposition, were imaged every 2 weeks for 60 days. Immediately after annealing, AgNWs processed at both temperatures visually looked similar under the SEM except for a waviness induced in the pressed nanowires due to the mechanical pressure. However, TEM imaging revealed that while the unannealed AgNWs had a 1-3 nm thick layer of PVP on their surfaces, this layer did not exist in the annealed sample.

Figure 3-9 compares the morphology of unannealed and annealed samples after two weeks of exposure to ambient conditions. There are only the beginnings of corrosion particle formation (particles < 10 nm in diameter) in the unannealed nanowires, whereas the annealed nanowires had larger (40 - 50 nm in diameter) and more numerous Ag_2S particles. This level of degradation observable in the annealed sample is parallel to the level of degradation observable in unannealed samples after 6 weeks of exposure to ambient. This trend continued, with the unannealed nanowires undergoing the same corrosion mechanisms as the annealed nanowires but at a much slower rate, explaining the slower rise in sheet resistance over time observed in Figure 3-1c.
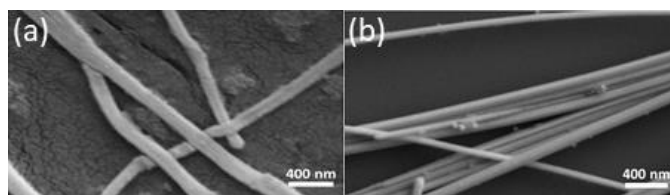
Figure 3-9: SEM images of silver nanowires after 2 weeks of exposure to ambient conditions. Nanowires were (a) pressed at room temperature and (b) annealed at 150 °C for 30 mins after deposition. Notice the lager corrosion particles on the surface of the annealed nanowires.

It was expected that annealing would accelerate degradation during the 30 minutes process, since both nanowire corrosion and instability are worsened at elevated temperatures [104, 103]. However, it was somewhat surprising that the 30 minute anneal accelerated degradation over the entire 60 day period, as evidenced by the higher slopes of the curves in Figure 3-2c. This may be because of increased silver atom diffusion at higher temperatures, and defects formed would increase reactivity with sulfur after the annealing, in turn leading to faster formation of Ag_2S. Small notches or bottlenecks in the nanowire, like in Figure 3-7c, may also be initiated during the annealing, and once these are formed further evolution into disconnections may be accelerated.

Another factor may be due to the reduction or removal of the PVP layer from the nanowire surface during anneals above ~150 °C (the exact temperature depends on the molecular weight of PVP used during nanowire synthesis) [125]. With less PVP, H_2S gas may be able to reach and adsorb on the silver surface more easily, and thus more corrosion would occur. This hypothesis echoes that of Elechiguerra et al. who hypothesized that a thicker layer of PVP on AgNWs would improve overall stability [110]. This hypothesis may also explain why the rate of degradation (related to the slope of the curves in Figure 3-1c) is higher for annealing temperatures above 150 °C compared to annealing temperatures of 80 °C and 120 °C, as the latter two conditions would not be high enough to significantly reduce the PVP layer.

Due to the lower rate of degradation, mechanically pressing a nanowire film at room temperature is an attractive alternative to annealing. At a transparency of 88% (wavelength = 550 nm), nanowires pressed on PET substrates have a sheet resistance of 23 $\Omega/\square$. This is similar to annealed electrodes on glass, and far superior to annealed electrodes on PET. The latter is because PET cannot tolerate temperatures above 100 °C since it permanently deforms. Nanowire electrodes annealed on PET at 100 °C have an average sheet resistance of approximately 300 $\Omega/\square$ at 87% transparency (wavelength = 550 nm). This high resistance can severely limit the end application of the AgNW electrodes. Mechanical pressing may also be a more convenient method than annealing to process AgNW films as not only is it roll-to-roll compatible, but is also quick (< 1 min) versus the ~30 mins required for an annealing process.

3.3.7. Effect of Plasma-Treated Substrates:

Plasma treatments increase the hydrophilicity of a substrate surface to aid in the adhesion of a subsequently deposited material without the need for chemical modification. They are commonly used for the preparation of AgNW electrodes to increase the adhesion of the

49

nanowires to glass or plastic substrates [69, 126, 96]. Corona plasma is a commonly used tool in the reel-to-reel processing industry because of its ease of use and non-destructive nature. Corona plasma is used to increase the hydrophilicity of a substrate surface (such as plastic or textile material) to aid in polymer adhesion to the specific substrate without any need of chemical modification [127]. Corona plasma is often used because it is an inexpensive and fast way to apply plasma treatments to plastic substrates without the need of a nitrogen blanket or inert atmosphere [127]. In the case of AgNWs, corona plasma was used in this work to promote adhesion to substrate without the need for any post-processing to reduce sheet resistance to below 50 $\Omega/\square$. It is suspected that corona plasma might soon be used with AgNWs to promote substrate adhesion to allow for high throughput fabrication of AgNW electrodes in the reel-to-reel industry.

In order to test the effects that corona plasma has on the corrosion rate of AgNWs, substrates first needed to be treated with the arcing plasma. A corona wand was held slightly above the sample to allow for a plasma arc to form between the sample and the wand. The substrate was then exposed to the plasma arc for approximately 10 seconds to ensure a thorough treatment of the entire substrate. AgNW electrodes were then fabricated using the procedure outlined in Chapter 2 of this document. Sheet resistances were monitored over the 60 day period to track any increases or changes in the electrical properties of the transparent electrodes.

Figure 3-1d shows the effect of corona plasma on the stability of AgNW electrodes. It was observed that the use of corona plasma significantly increases the sheet resistance over a period of 60 days after exposure to ambient conditions (increase of over 4x an unprocessed electrode). This phenomenon is hypothesized to be because of the increase in hydrophilicity of the substrate. The increased hydrophilicity of the substrate caused by the corona treatment leads

to a higher buildup of surface water. Graedel reported on the increased rate of corrosion on silver in humid environments [31]. Surface water provides a medium for the absorption of corrosion-causing gases as well the dissolution of silver ions and therefore increases corrosion rates [108]. It is well known that AgNWs degrade faster in humid environments [107, 104].

It can therefore be concluded that the use of corona plasma to increase the adhesion of AgNWs to the surface of a substrate can cause a significant increase in sheet resistance over a short period of time. The hydrophilic nature of the substrate caused by corona plasma treatment is considered to be the major factor involved in the higher corrosion rate, as the hydrophilic surface allows for increased adsorption of H_2S by the AgNW electrode [107, 104]. It would be wise for transparent electrode designers to avoid surface treatments that cause the substrate to be more hydrophilic if they choose to use AgNWs as a transparent electrode material. Instead, the use of room-temperature pressing is once again recommended as an alternative treatment to both lower sheet resistance and increase adhesion of the NWs to the substrate [93, 128]. It is suspected that annealed samples that were subjected to corona plasma treatment would have significantly higher corrosion rates because of the effects of the hydrophilic substrate. More work will need to be conducted to investigate this theory, as the PVP layer on the room-temperature fabricated electrodes could slow the degradation caused by the corona plasma treatment- as annealed samples without a PVP layer would be subjected to a faster adsorption of H_2S because of this increased hydrophilicity.

3.3.8. *Corrosion Rates at Low Vacuum conditions*

Based on the results observed in the above sections, one can observe that AgNWs undergo degradation when exposed to ambient- resulting in the 3 observations made in Figure 3-2. However, only one of the observations made above can be related to a classical tarnish caused

by Ag_2S formation on the AgNW surface. The phenomenon of particle formation causing nanowire bisection is only a phenomenon observed in AgNWs with very small diameters (i.e. <40 nm), while the formation of large agglomerations appears to be a phenomenon only observed in dense AgNW networks. Determination of the causes of these two phenomena is important, as they may be morphological instabilities inherent of a nanowire structure (e.g. Rayleigh instability) [103], or be true corrosion artifacts only caused after exposure of the AgNW to H_2S in ambient. If the phenomena witnessed are determined to be morphological instabilities, it may be the case that AgNWs under a certain diameter are inherently unstable.

In order to address this issue, four AgNW electrodes were fabricated in the same manner using Novarials A20 20 nm nanowires and placed in a low vacuum environment (after purging with nitrogen 3 times) for 60 days, and compared directly to AgNW electrodes fabricated using the same nanowires on the same day- but stored in ambient conditions. Sheet resistances of both types of electrodes were monitored periodically to observe the changes over time (Figure 3-10, Figure 3-11, Figure 3-12). Furthermore, SEM images of the nanowires were taken after the 60 days in vacuum to act as a visual inspection for nanowire instability (Figure 3-13).
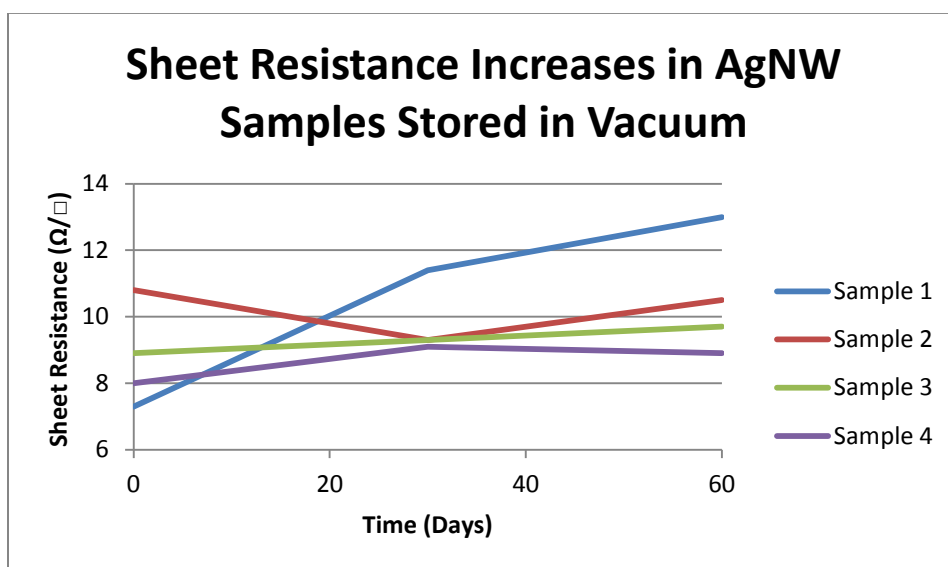
Figure 3-10: Tracking the change in Rs of Novarials A20 samples stored in vacuum for a period of 60 days.

The change in sheet resistance over the 60 day period is recorded in Figure 3-10 amongst 4 samples in vacuum, with the percentage change available in Figure 3-11. Based on these two plots, it is evident that there is some sheet resistance increase in the samples stored in vacuum (minimum increase is 9%, maximum increase is 74% - Sample 2 was omitted because of a negative increase in sheet resistance attributed to variability in measurement from the digital multimeter). After accounting for the consistency of contact between the digital multimeter and sample, one can see that there is a slight increase in sheet resistance over time. However when compared to the samples left in ambient conditions, one can see that the sheet resistance increases in vacuum are negligible compared to the sheet resistance increases of electrodes left in ambient (Figure 3-12). The sheet resistance of the ambient-stored electrodes increased by 174% in a period of 60 days, while the sheet resistance of the electrodes stored in vacuum only reached a maximum increase of 74%. Clearly the presence of H_2S is a much more significant factor to take into consideration than the increases attributed to the nanowires sitting in vacuum.
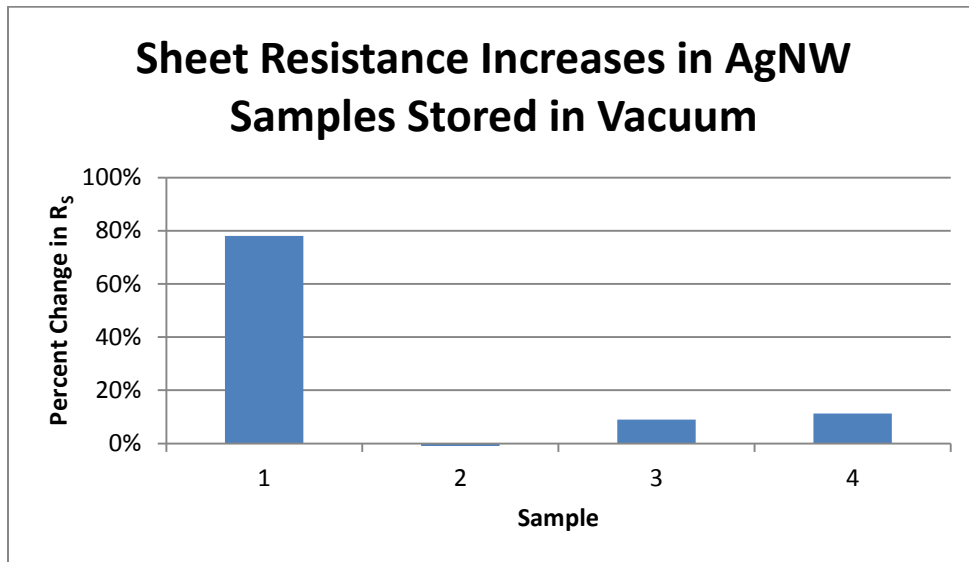
Figure 3-11: Showing the percent increase of Rs in Novarials A20 samples placed in vacuum for 60 days.
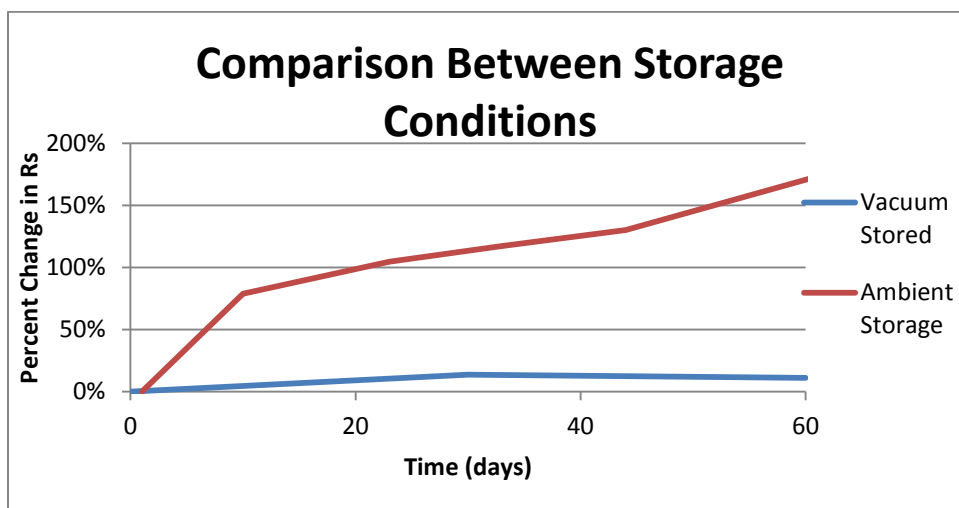
Figure 3-12: Comparison between the average sheet resistance increases of AgNW electrodes stored in ambient conditions vs electrodes stored in a low vacuum environment
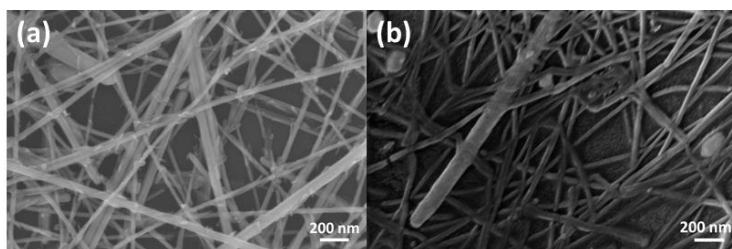
Figure 3-13: (a) SEM images of Novarials A20 AgNWs left for 60 days (a) in ambient, exhibiting corrosion effects. (b) SEM images of AgNWs left in vacuum for 60 days showing very little corrosion effects in a dense network

Based on the data observed in Figures 3-10 and 3-11, it is clearly evident that the content of the atmosphere plays a significant role in the instability of AgNWs. Because the low vacuum condition still contains trace amount of atmospheric air, it can be hypothesized that it does contain some amount of H_2S. However, this concentration of H_2S in low vacuum is negligible when compared to the concentration of H_2S in an atmospheric condition. However, the increasing sheet resistance in Figure 3-11 and Figure 3-12 state that there must be some discontinuity in the nanowire network- otherwise the sheet resistance would not increase. It is postulated that the instabilities observed in small diameter nanowires as stated above are still relevant to electrodes stored in low vacuum conditions. The increase in sheet resistance in the

presence of negligible H_2S can still be attributed to instabilities in the nanowire, but degradation due to instability occurs at a much faster rate when the AgNWs are undergoing corrosion in an atmospheric condition. The major conclusion that can be made from this study is that the atmosphere clearly plays a role in the instability of AgNWs. AgNW instability is much more common in an atmospheric condition- meaning that corrosion accelerates the formation of instabilities in small diameter AgNWs. It is hypothesized that the corrosion occurring on the small diameter AgNWs causes the nanowire body to become thinner (as Ag diffuses and Ag_2S forms along the nanowire body)- giving the AgNWs a much higher instability due to the increased surface to volume ratio. This increased SA/V ratio of corroded AgNWs makes them much less stable than original diameter AgNWs- which eventually leads to a faster increase in sheet resistance over a given time period.

3.4. Conclusions

Our results show that common variations in the composition and processing of silver nanowire electrodes, namely nanowire diameter, nanowire density, annealing temperature, and substrate plasma treatment, significantly increase the rate of electrode degradation. This explains some of the large variation of sheet resistance increases from one report to the next. Regarding the nanowire electrodes mentioned in section 1.4.3, Mayousse's electrodes, which were the ones with long lifetimes, were annealed at a low temperature of 80 °C compared to 140 °C for both Moon and Vaagensmith [67, 69, 74]. Jiu instead used high intensity pulsed light to sinter the AgNW networks which causes silver to eject electrons via the photoelectric effect, resulting in a faster rate of corrosion due to the formation of Ag^+ ions [65, 129]. The Mayousse electrodes were also quite dense. Through image processing of images provided in their papers, the Mayousse nanowire density was 27 mg/m^2 compared to 5 and 17 mg/m^2, respectively, used by

Vaagensmith and Jiu. All five previous studies mentioned in the introduction used different nanowire diameters. And lastly, Moon and Vaagensmith used a plasma treatment whereas the other researchers did not. These factors are all in addition to environmental differences between the various studies which are known to have significant effects on corrosion rates; Vaagensmith, Jiu and Mayousse stored their nanowires in ambient laboratory air while the samples of Elechiguerra and Moon were exposed to elevated humidity and temperature conditions.

In addition to explaining varying degradation rates, this study also gives guidance on how to design electrodes with longer lifetimes. According to our results, electrodes consisting of dense networks of larger diameter nanowires that are processed at room temperature and are not exposed to corona plasma should fare better than other electrodes. Regarding the latter two variables, mechanical pressing is an alternative option to both annealing and corona plasma treatment, since pressing both welds nanowire junctions as well as increases nanowire adhesion to plastic substrates [93, 128]. Regarding dense and thick nanowires, this may not always be possible due to design considerations. Denser nanowire films result in lower transparencies, and larger diameter nanowires lead to more haze which is undesirable for certain applications such as display technologies. If nanowire diameters less than 40 nm are used, our study suggests that in addition to passivation layers which block corrosion-causing gases, strategies to increase their morphological stability may be helpful.

Regardless of the electrode composition and processing conditions, our results show that some degradation will still occur and an effective passivation strategy will still be necessary. For many applications, the passivation layer needs to be both transparent and conductive, block gas, be mechanically flexible, and cost effective. Although many passivation materials have been

studied, more work needs to be done before AgNW electrodes can be used as a viable ITO

replacement in a range of applications.

Chapter 4:   Silver Nanowire Electrode Passivation using Phenyl Capped Aniline Tetramer

4.1. Introduction

As discussed earlier in Chapter 3 that although the silver nanowire diameter, density and processing procedures of the AgNWs in electrodes can be optimized to reduce degradation, we still can observe the corrosion effect, and additional passivation required before they can be used in commercial devices. Many passivation materials are currently suggested in the literature. Attempts such as Ag/Ni core-shell nanowires [75], bioactive polymers [130], zinc oxide [131, 132, 133], titanium oxide [134], graphene oxide [79] and even photoresist [135] have been extensively studied as possible passivation materials for AgNW electrodes. However, the suggested passivation materials still need more improvement due to several reasons as follows: Firstly, each one of these passivation materials still allows for some increase of sheet resistance over an extended period of time. Secondly, all the passivation layers negatively affect both the sheet resistance and transparency of the AgNW network. Thirdly, many of the passivation layers are not deposited in solution nor are mechanically flexible, negating some of the advantages of AgNW electrodes.

A passivation layer should be optimized depending on the required application of the silver nanowire electrode. For example, many optoelectronic devices including OLEDs and organic solar cells, the current needs to flow to or from the AgNW electrode into the active layers of the device. Therefore, the passivation layer needs to be electrically conductive itself, or extremely thin such that electrons can tunnel across it. Passivation layers such as bioactive polymers and photoresist, regardless of their effectiveness in slowing corrosion, are unlikely to be used as passivation materials in such devices because of their non-conductive character.

For conventional bulk or thin-films of metals that corrode, there exist electrically conductive coatings that act as a barrier to corrosion [136, 137]. It has been observed that polyaniline (PANI) coatings can remain corrosion inhibitive even when the coating has been scratched through to the underlying metal [138, 139, 140]. Research shows that the PANI chemically interacts with the metal it is being deposited on, and acts similarly to a sacrificial anode. A sacrificial anode is a highly active metal that is used to prevent a less active material surface from corroding. Sacrificial anodes are created from a metal alloy with a high negative electrochemical potential, which will be consumed in place of the metal, it is protecting. As an example, a thin layer of zinc on a steel surface acts as a corrosion preventative mechanism, as the zinc coating acts as a sacrificial anode when the underlying steel is exposed [141]. Because of this revelation, and its ease of deposition, PANI is widely used today as an anti-corrosion material on many surfaces prone to corrosion [142].

Oligomers have been reported to possess corrosion-inhibiting properties that are superior to PANI itself [142]. Furthermore, because oligomers have much lower chain lengths than polymers, a smaller volume is needed to protect the surface, meaning that it wouldn't decrease transparency as much as a high molecular weight polymer. It has been observed that phenyl capped aniline tetramer (PCAT) and other oligomer forms of polyaniline have excellent anti-corrosion properties when deposited on steel and iron samples, as the C=N functional grouping on the oligomer readily adsorbs onto iron oxides, preventing further oxidation via its resonant structures. A structure of PCAT is included in Figure 4-1 [143].
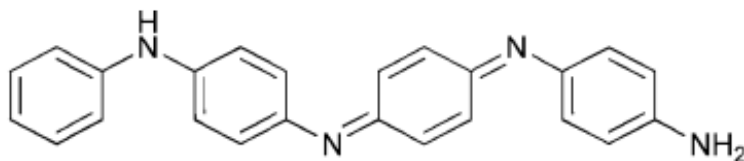
Figure 4-1: Molecular structure of PCAT [143].

Because PCAT is very effective on the surface of iron as a corrosion passivating material, and because it is a transparent and conducive material on its own, it was recommended that the same material be used on AgNW electrodes as a potential corrosion passivation layer. Furthermore, PCAT is cost effective material that has the potential to be solution deposited, and is mechanically flexible. Lastly, it has the potential to be deposited on the surface of the nanowires before they are deposited as film. This would allow for no passivation material being needed on the substrate between the nanowires, which would interfere with their transparency even less. If PCAT could be verified as an acceptable passivation material such that minimal increase in sheet resistance occurs and the transparency and conductivity of the AgNW electrode is not significantly altered, it could represent a potential major breakthrough to the incorporation of AgNWs as transparent electrodes in materials such as OLEDs, LEDs, and solar cells.

4.2. Experimental Details

PCAT was obtained from Professor Peter Kruse's group at McMaster University in Hamilton, Ontario. The Kruse group synthesized the PCAT in lab to have a MW of 422.22 g/mol. First, the Solubility of PCAT in an organic solvent is determined in order to allow for solution processing methods of this thin aniline tetramer layer. Because the nanowires were dispersed in ethanol, and to avoid any density mismatches or solvent incompatibilities, PCAT was dispersed in ethanol. If PCAT polymer were not soluble in any common organic solvents, the following procedures would not have been feasible, resulting in the application of PCAT

onto the silver nanowire electrode surface using physical deposition techniques such as thermal evaporation.

5.0 g of ethanol is mixed with 20 mg of PCAT in a 20 mL sample vial, which is then capped and stirred via a stir-plate for 1 hour to completely dissolve the tetramer. After PCAT was fully dissolved (via visual inspection), an additional 10 mg was added and left to stir in the 5.0 g of ethanol for approximately 1 hour. This procedure was repeated until a total of 50 mg of PCAT was added to the solution of ethanol as at this point, there appeared to be small precipitates of PCAT in the bottom of the sample vial. The vial was then left to stir for 3 additional hours to allow for dissolution time, after which no PCAT solid was visible in the sample vial. The final concentration of the solution was calculated to be 7.8 mg/mL of PCAT in ethanol. This was the stock solution used for the remainder of the investigation.

All silver nanowire electrodes were prepared via the Mayer rod coating method. 5 x 4 cm glass and polyethylene terephthalate (PET) substrates were cleaned using acetone, isopropanol, and water in a sonicating bath and blown dry with a nitrogen gun to remove dust and any surface contaminants. 40 µL of 4 mg/mL AgNWs in ethanol (Novarials A20, average diameter and length of 20 nm and 20 µm, respectively) was pipetted onto a glass or PET substrate. A clean RDS 10 Mayer rod was then rolled across the surface to evenly deposit a thin layer of silver nanowires on the substrate. The substrate was then left to dry for 2 minutes, and then the deposition was repeated, with the Mayer rod being rolled in the opposite direction across the substrate. Nanowires deposited on PET were then mechanically pressed at room temperature using a rolling system (MSK-HRP-01, MTI Corporation, Richmond, USA), twice with a roller spacing of 70 µm and then twice more with a spacing of 60 µm. Nanowires deposited on glass were annealed at 150°C for 30 minutes to fuse the nanowire junctions and aid in removal of any

organic layers on the nanowire surface. Silver paste was then applied across the top and bottom of the electrode to complete a circuit.

For a proper comparison, a different set of experiments is designed including the use of thick-vs-thin layers of PCAT, temperature treated-vs-pressed, and pre-coating of silver nanowires with PCAT before film deposition vs after, a variety of samples were fabricated (Table 4-1). Based on the procedure for depositing nanowires listed previously, the following samples were prepared for testing:

Table 4-1: Summary of experimental conditions when fabricating electrodes with PCAT encapsulation layers

Sample	Experimental Condition
1. Glass Control (Annealed at 150C, 30 min)	Novarials A20 AgNWs were Mayer rod coated on a glass substrate. The substrate was then annealed at 150°C for 30 minutes. No PCAT was deposited onto this sample.
2. PET Control (AgNWs pressed on PET)	Novarials A20 AgNWs were Mayer rod coated on a PET substrate and subjected to mechanical pressing. No PCAT was deposited onto this sample.
3. Glass Substrate- Dropcast PCAT (thick layer)	Novarials A20 AgNWs were Mayer rod coated on a glass substrate. The substrate was then annealed at 150°C for 30 minutes. A ~100 μm thick layer of PCAT was drop-cast onto the AgNW coated glass substrate. The entire device assembly was then annealed at 50°C for 30 minutes.
4. Glass Substrate- RDS 10 PCAT layer thickness	Novarials A20 AgNWs were Mayer rod coated on a glass substrate. The substrate was then annealed at 150°C for 30 minutes. A 10 μm thick layer of PCAT was Mayer rod coated onto the AgNWs. The entire device assembly was then annealed at 50°C for 30 minutes.
5. PET Substrate- Dropcast PCAT (thick layer)	Novarials A20 AgNWs were Mayer rod coated on a PET substrate and subjected to mechanical pressing. The substrate was then left to dry for 30 minutes. A ~100 μm thick layer of PCAT was drop-cast onto the AgNW covered PET substrate. The entire device assembly was then annealed at 50°C for 30 minutes to evaporate any solvent.
6. PET Substrate- RDS 10 PCAT layer thickness	Novarials A20 AgNWs were Mayer rod coated on a PET substrate and subjected to mechanical pressing. The substrate was then left to dry for 30 minutes. A ~100 μm thick layer of PCAT was drop-cast onto the AgNW covered PET substrate. A 10 μm thick layer of PCAT was Mayer rod coated onto the AgNWs. The entire device assembly was then annealed at 50°C for 30 minutes.
7. PCAT: AgNW (4.8:4 mg/mL) Pressed	1 mL of Novarials A20 AgNW solution (4 mg/mL solution concentration) and 1 mL of PCAT dissolved in ethanol (4.8 mg/mL) were combined and mechanically stirred for 3 hours at ambient temperature. The mixed solution was then Mayer rod coated on a PET substrate and mechanically pressed at room temperature.

All nanowire electrodes were left in a 40% relative humidity environment at 22.5 °C (+/- 2% variance on both temperature and humidity) for a 28 day period, with sheet resistance of the electrodes being measured every week using a multimeter. Transparency at 550 nm was also monitored using a handheld SRW 2000 Window Tint Meter to observe if there was any degradation occurring in the PCAT layer during the test period. Furthermore, to test the viability of PANI as a transparent electrode passivation layer for AgNWs, it was electrodeposited using a weak HCl solution onto glass AgNW electrodes. However, after electrodeposition the electrodes were non-conductive. It is hypothesized that the HCl used to allow for polymerization lead to the formation of AgCl, which in turn caused discontinuities in the AgNW network- as AgCl is not electrically conductive. Therefore, characterization of these samples was not pursued further.

4.3. Results and Discussion

Table 4-1 and Figures 4-2, 4-3, and 4-4 state the results observed during the PCAT study. It was observed that the use of PCAT as a passivation material had a negligible effect on the passivation of AgNW electrodes.

Table 4-2: Results of the PCAT study as a passivation layer for AgNW transparent electrodes.

Sample	Sheet resistance (ohms/square)	Transparency (%)	Day: 1	7	13	19	25	28	Percent Increase in Sheet Resistance	Transparency on day 28
1. Glass Control (Annealed at 150C, 30 min)	101.2	87.9	101.2	120.2	135.1	151.3	513.1	1631	**1612%**	87.8
2. PET Control (AgNWs pressed on PET)	70.2	85	70.2	86.6	100.3	116.6	5136	13670	**19473%**	85.1
3. Glass Substrate-Dropcast PCAT (thick layer)	66.7	75.9	66.7	77.9	88.4	93	7861	1E+11	**INF**	76.1
4. Glass Substrate-RDS 10 PCAT layer thickness	58.6	78.7	58.6	66.6	78.9	94.7	516.5	1844	**3147%**	78.5
5. PET Substrate-Dropcast PCAT (thick layer)	85	75	85	94.6	124.3	136	843	1834	**2158%**	75.3
6. PET Substrate-RDS 10 PCAT layer thickness	94.3	76.8	94.3	110	112.3	137.9	424	2322	**2462%**	76.4
7. PCAT: AgNW (4.8:4 mg/mL) Pressed	101.1	73.8	101.1	803	5972	8010	32560	1E+11	**INF**	73.2
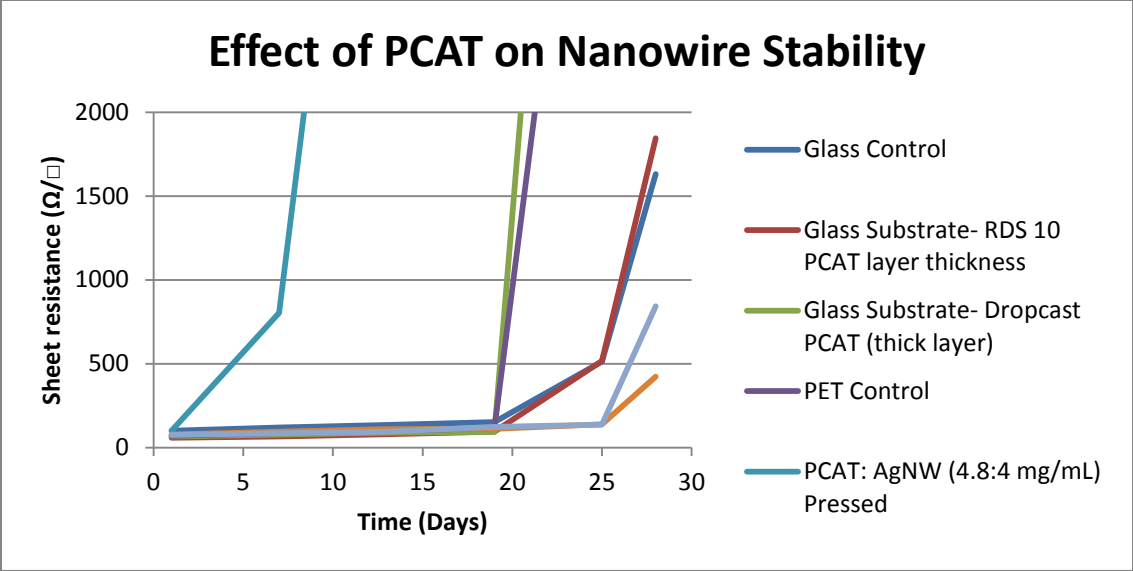
Figure 4-2: The effect of PCAT on Nanowire stability after AgNW networks were exposed to ambient conditions for a period of 28 days. It should be noted that the control samples of glass and PET did not corrode as quickly as any sample coated with PCAT.
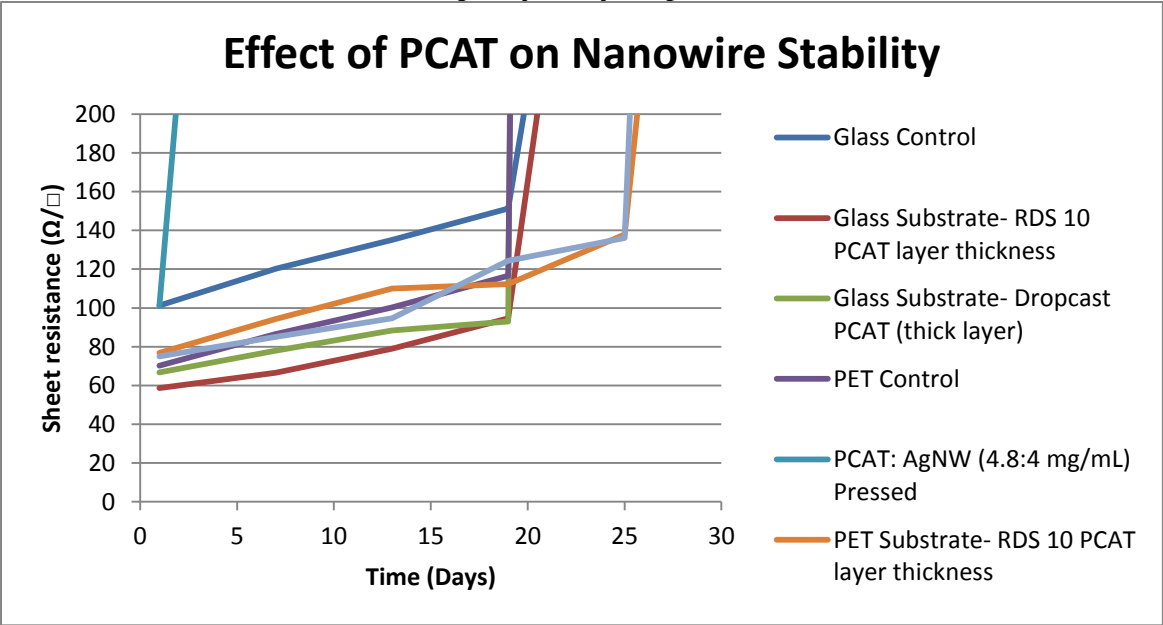
Figure 4-3: This graph shows the effects of PCAT on AgNW transparent electrodes. It is the same information as Figure 4-1, but only displays sheet resistances below 200 Ω/□

Effect of PCAT on Nanowire Stability

Sheet resistance (ohms/square)

1631 ohms/square

1844 ohms/square

Open

13760 Ohms/square

Open

2322 Ohms/square

1834 Ohms/square

Day 1
Day 30

Glass Control (Annealed at 150C, 30 min) — Glass Substrate- RDS 10 PCAT layer thickness — Glass Substrate- Dropcast PCAT (thick layer) — PET Control (AgNWs pressed on PET) — PCAT: AgNW (4.8:4 mg/mL) Pressed — PET Substrate- RDS 10 PCAT layer thickness — PET Substrate- Dropcast PCAT (thick layer)

Electrodes Created

Figure 4-4: Starting and final resistances of the electrode samples after the completion of the study. As the graph displays, the final sheet resistances of the PCAT coated electrodes were much higher than the control study, indicating its ineffectiveness as a passivation layer.

Based on the recorded results during the study, one can see that the addition of PCAT did not prevent nanowire degradation. On glass substrates, it even seemed to increase the rate of degradation. Although the C=N functional group on the PCAT structure was readily adsorbed by iron oxide films, it is hypothesized that the PCAT layer did not undergo any physical adsorption due to the presence of polyvinylpyrollidone (PVP) on the silver nanowire surface. The PVP on the AgNW body could prevent the C=N functional group from contacting the Ag on the surface of the nanowire. To test this hypothesis, a future experiment could be performed to remove the

PVP from the AgNW surface before the PCAT is deposited. PVP can be removed from the surfaces of AgNWs by annealing at 200°C for 30 minutes **[92]**, and then depositing PCAT onto the surface of the AgNWs. Another inefficiency of PCAT as a passivation layer is that PCAT might not readily absorb onto the surfaces of AgNWs is due to a lack of significant oxygen atoms on the surface of Ag since, as was discussed in Chapter 3, AgNWs do not form a native oxide. For a Fe surface, we know that it is the oxygen atoms that PCAT reacts strongly with **[143]**.

Even more, the poor performance of PCAT as a passivation layer may be explained as follows: It has been previously observed that the use of transparent organic coatings as corrosion inhibition layers on silver electronics (not necessarily silver nanowires) can trap moisture between the organic layer and nanowire surface [144, 145, 146]. An increase in humidity will increase the rate of degradation because the presence of surface water is likely to increase the amount of hydrogen sulfide absorbing onto the surface of the nanowire, causing instability, silver sulfide growths, and defects along the conducting network [68].

It should also be noted that there is a physical limit when mixing PCAT and AgNW solutions together before film deposition. In addition to successfully mixing PCAT with Novarials A20 20 nm diameter AgNWs, attempts at mixing Novarials A70 70nm diameter AgNWs with PCAT solution were made. However, the PCAT and AgNWs coalesced in solution and precipitated. This did not allow for an even deposition of AgNWs on the substrate and resulted in open circuit electrodes from the first set of measurements. This difficulty in mixing larger diameter AgNWs with PCAT was also shared with a labmate Alexandra Madeira, as the labmate attempted mixing 70 nm AgNWs with another small molecule (11-Mercaptoundecanoic acid) and had a similar agglomeration effect.   Perhaps the larger diameter AgNWs have

difficulties with adsorption of small molecules because of their PVP coating, or the negligible charge of the AgNW. However, it is hypothesized that the absorption of small molecules onto smaller AgNWs has a much more prominent result because of their high surface-area to volume ratio. A higher surface area-to-volume ratio in small diameter AgNWs allows for a much higher surface energy leading to a higher adsorption rate than a nanowire with a larger (i.e. 70 nm) diameter. This mechanism perhaps states that there is a size limitation on AgNWs if they are to be mixed with PCAT for future testing. Future experiments using small molecules could perhaps occur if the AgNWs were under current. Perhaps the current flowing through the AgNWs would allow for an easier binding of small molecules to the body of the nanowire.

4.4. Other Attempts Passivation Layer Optimization

A UV curable polymer based on pentaerythritol triacrylate and a bis-acylphosphine oxide (BAPO) photoinitiator was tested as a potential passivation layer. This experiment involved a AgNW based electrode using Novarials A20 nanowires that were pressed into a PET substrate as outlined in chapter 2The UV curable formation was then mixed and dispersed in ethanol at a 30 wt% concentration to allow for ease of deposition. The UV curable polymer was then Mayer-rod coated across the AgNW electrode and allowed to cure in a mercury arc lamp for 3 seconds before being removed and tested for completeness of the polymerization. Sheet resistances were observed for the same 30 day period as the PCAT samples to check for deviations in the corrosion rate of the AgNWs. It was discovered that the UV cured samples did not degrade as quickly as the PCAT or control samples, but still had sheet resistance increases of approximately 4X over the same period. This means that the although the this UV curable formulation could be optimized to extend the lifetime of the AgNW electrodes used, it likely cannot offer a full solution to the ongoing issue of AgNW corrosion due to the trapping of moisture next to the

AgNWs [146]. Furthermore, the non-conductive nature of the UV curable formulation proposed limits the possible applications of this style of AgNW transparent electrode.

4.5. Conclusions

A set of experiments attempted to test a possible passivation layer in the form of a phenyl-capped aniline tetramer commonly referred to as PCAT. It can be concluded that PCAT is an unsuitable passivation material because it did not prevent the increase in sheet resistance of the AgNW networks it was deposited onto, regardless of the deposition or mixing method. The sheet resistance of AgNW electrodes coated with PCAT increased more than 2000% when left in atmosphere for 28 days. Based on the results observed, further investigation is required to develop a suitable passivation method for AgNWs electrodes.

Future work could also be conducted related to encapsulation of AgNWs with inorganic and hydrophobic materials. Materials such as SiO_x would be effective as passivation layers because of their hydrophobic and encapsulating properties. Hydrophobic materials such as treated polydimethylsiloxane would also be effective passivation layers to prevent the trapping of water monolayers against the AgNWs. As long as the inorganic or hydrophilic materials are compatible with potential device architectures (i.e. remain conductive after deposition), they could be considered effective passivation layers for AgNW electrodes.

Chapter 5: Conclusions and Future Work

5.1. Summary and Contributions

This thesis studies the problematic behaviour of silver nanowire degradation in transparent electrodes. This topic has been addressed before in a few studies [147] [68] [79] [74] [148], However, our present work succeeded to offer novel contributions as follows: While previous studies performed in this area only investigate the effect of environmental factors such as light and humidity on nanowire electrode resistance over time, this work focuses on the detailed examination of nanowire film composition and the processing parameters involved in the electrode fabrication process. While many parameters tested had no significant effect on nanowire degradation, nanowire diameter, density, the annealing temperature used and substrate plasma treatment had a major effect on the silver nanowire electrode lifetime. Secondly, other studies attribute silver nanowire degradation to corrosion Induced by silver nanoparticles on the nanowire surface. Similar observations were found with larger diameter nanowires (> 40 nm), however for smaller nanowire diameters (<40 nm) we proposed a new mechanism of silver nanowire degradation. Corrosion was not the main artifact observed in these samples, but evidence instead suggests it was the transition of the nanostructures by diffusing silver, leading to discontinuities in the nanowire network- causing the electrode sheet resistance to increase. Knowing that morphological instability can play a role in electrode breakdown may allow engineers to better design a passivation solution for thin nanowire networks as corrosion is not the only concern. Lastly, phenyl capped aniline tetramer (PCAT) was investigated in chapter 4 for the first time as a passivation material for silver nanowires. It was found that PCAT is not effective as a passivation material, concluding that future work is needed in regards to discovery of an effective passivation layer for AgNW electrodes. Overall, the work conducted in this thesis

provides useful information to guide future researchers towards solutions to mitigate corrosion in silver nanowire electrodes, and suggests solutions for their lifetime.

5.2. Recommendations to Extend the Lifetime of Silver Nanowire Electrodes

As learned from the work conducted in this thesis, a list of recommendations can be suggested for increasing the silver nanowire based transparent electrode lifetime

- Silver nanowires of larger diameters (i.e. > 40 nm)are strongly recommended in order to to reduce the possibility of morphological instabilities causing discontinuities in the nanowire network.

- Highly dense silver nanowire networks offer continuous conductive pathways for current to flow. The sheet resistance of a dense nanowire network will increase much more slowly than a sparse nanowire network.

- Room temperature post treatment methods such as using a rolling press are highly preferable compared to thermal treatment methods in order to achieve silver nanowire networks with low sheet resistances [93].

- Plasma post treatment is not recommended for increasing the substrate adhesion properties due to the increased hydrophilicity of the substrate- allowing for faster formation of Ag_2S. Instead, room temperature pressing and/or chemical treatments of the surface are strongly suggested due to no effects being imparted onto the hydrophobic or hydrophilic properties of the substrate [93] [149, 150].

5.3. Future Work

The main challenging problem found so far is to develop an effective passivation layer for silver nanowire electrodes. The passivation layer should acquire some important features including:

- It must successfully prevent sulfidization on the surface of the silver nanowire electrodes. Formation of Ag_2S on the surface of the silver nanowires can cause increases in sheet resistance, breaks in the silver nanowire electrode, and discolouration (i.e. yellowing) of the electrode body.

- For applications including solar cells and OLEDs, the passivation layer itself should be optimized wisely to maintain the conductivity so current can pass between the electrode and the active layers.

- It should not affect the transparent characteristics of the silver nanowire electrodes. In order for successful device integration, the passivation layer deposited onto the silver nanowire electrodes must have a transparency equal to that of ITO, and in the case of display technologies, have a haze of <2%.

- The optimum passivation layer should be scalable under the current manufacturing environment (film manufacturer). Therefore, it should ideally not be applied to the silver nanowires via physical deposition methods (vapour deposition, CVD, sputtering, etc.). Instead methods of solution processing such as spin-coating and Mayer rod deposition, which allows for scalability on reel to reel manufacturing. Furthermore, the passivation layer must be cost effective for the sake of adoption in industry.

Recently, different passivation techniques were suggested to improve AgNW electrode passivation solutions. One aspect of passivation layers that have not yet been studied is the effect

of passivation layer deposition temperatures. Passivation materials such as Ni and Al have been deposited using sputtering or thermal evaporation which are done at temperatures higher than (or around) 800°C [75]. We know from the results of this thesis that AgNW films exposed to elevated temperatures even for a short time can affect long-term degradation rates. Thus, future work should study whether higher passivation material deposition temperatures negatively affect AgNW electrode resistance over time, and whether lower deposition temperatures can be used to make passivation materials more effective.

Another aspect regarding passivation layers that arises from this work is that the passivation layer should not only protect the AgNWs from corrosion, but it also must prevent morphological instabilities of the AgNWs. This study revealed that morphological instabilities of AgNWs are a mechanism of degradation that causes nanowire networks to become discontinuous. Thus the passivation of both corrosion and AgNW instabilities must be addressed with future study. A different approach to mitigate the instability problem is to develop a method to synthesize AgNWs with lower energy facets, such as {111} compared to the higher energy {100,such lower surface energy AgNWs would be less energetically driven to reorganize and thus be more stable.

Another future study would involve synthesizing silver nanowires using a polyol process to make them corrosion resistant and thus not needing an additional passivation layer. For conventional bulk and thin-films of silver, typically a chromium-silver, gold-silver, or palladium-silver alloy is employed in industry as a method of eliminating the rate of corrosion of silver plating [151, 152, 153]. If there is a way to incorporate an alloyed nanowire using gold-silver, chromium-silver, or palladium-silver, perhaps the corrosion problem of AgNWs in ambient environments would be eliminated in its entirety. This idea would only work if the conductivity

of the final material would not be significantly affected, and the electrodes formed from these nanowires would still maintain the same transparency as current silver nanowire networks.

The future studies of a passivation layer and an alloyed nanowire structure are believed to be the next logical steps for completely eliminating the corrosion issue in nanowire structures made of silver.

Bibliography

[1]   J. Fenn, "If not ITO, then what?," in *Society of Vacuum Coatings*, Orlando, 2010.

[2]   Solid State Technology: Insights for Electronics Manufacturing, "Transparent electrode market to grow $5.1 billion by 2020," Solid State Technology, 1 May 2013. [Online]. Available: http://electroiq.com/blog/2013/05/transparent-electrode-market-to-grow-to-5-1-billion-by-2020/. [Accessed 9 March 2017].

[3]   J. Robertson and B. Falabretti, "Electronic Structure of Transparent Conductive Oxides," in *Handbook of Transparent Conductors*, New York, Springer Science and Business Media LLC, 2011, pp. 27-50.

[4]   A. Kumar and C. Zhou, "The Race to Replace Tin-Doped Indium Oxide: Which Material will Win?," *ACS Nano,* vol. 4, no. 1, pp. 11-14, 2010.

[5]   P. Edwards, A. Porch, M. Jones, D. Morgan and R. Perks, "Basic materials physics of transparent conducting oxides," *Dalton Transactions,* no. 19, pp. 2995-3002, 2004.

[6]   D. Langley, G. Giusti, C. Mayousse, C. Celle, D. Bellet and J.-P. Simonato, "Flexible transparent conductive materials based on silver nanowire networks: a review," *Nanotechnology,* vol. 24, pp. 1-20, 2013.

[7]   R. G. Gordon, "Criteria for Choosing Transparent Conductors," *MRS bulletin,* pp. 52-57, 1 August 2000.

[8]   Z. Wu, Z. Chen, X. Du, J. M. Logan, J. Sippel, M. Nikolou, K. Kamaras, J. R. Reynolds, D. B. Tanner, A. F. Hebard and A. G. Rinzler, "Transparent, Conductive Carbon Nanotube Films," *Science,* vol. 305, pp. 1273-1276, 2004.

[9]   E. M. Doherty, S. De, P. E. Lyons, A. Shmeliov, P. N. Nirmalraj, V. Scardaci, J. Joimel, W. J. Blau, J. J. Boland and J. N. Coleman, "The spatial uniformity and electromechanial stability of transparent, conductive films of single walled nanotubes," *Carbon,* vol. 47, pp. 2466-2473, 2009.

[10]   M. Zhang, S. Fang, A. A. Zakhidov, S. B. Lee, A. E. Aliev, C. D. Williams, K. R. Atkinson and R. H. Baughman, "Strong, Transparent, Multifunctional, Carbon Nanotube Sheets," *Science,* vol. 309, pp. 1215-1219, 2005.

[11]   M.-G. Kang and L. J. Guo, "Nanoimprinted Semitransparent Metal Electrodes and Their Application in Organic Light-Emitting Diodes," *Advanced Materials,* vol. 19, pp. 1391-1396, 2007.

[12] G. Eda, G. Fanchini and M. Chhowalla, "Large-area ultrathin films of reduced graphene oxide as a transparent and flexible electronic material," *Nature Nanotechnology,* vol. 3, pp. 270-274, 2008.

[13] V. C. Tung, L.-M. Chen, M. J. Allen, J. K. Wassei, K. Nelson, R. B. Kaner and Y. Yang, "Low-Temperature Solution Processing of Graphene-Carbon Nanotube Hybrid Materials for High-Performance Transparent Conductors," *Nano Letters,* vol. 9, no. 5, pp. 1949-1955, 2009.

[14] X. Wang, L. Zhi and K. Mullen, "Transparent, Conductive Graphene Electrodes for Dye-Sensitized Solar Cells," *Nano Letters,* vol. 8, no. 1, pp. 323-327, 2008.

[15] S. De, T. M. Higgins, P. E. Lyons, E. M. Doherty, P. N. Nirmalraj, W. J. Blau, J. J. Boland and J. N. Coleman, "Silver Nanowire Networks as Flexible, Transparent, Conducting Films: Extremely High DC to Optical Conductivity Ratios," *ACS Nano,* vol. 3, no. 7, pp. 1767-1774, 2009.

[16] R. Gupta, "Silver Nanowire Electrodes: Enabling Flexible, Transparent and Cost Effective OLED Lighting," in *DOE SSL R&D Workshop*, San Francisco, 2015.

[17] C. Gao, Z. Guo, J.-H. Liu and X.-J. Huang, "The new age of carbon nanotubes: An updated review of functionalized carbon nanotubes in electrochemical sensors," *Nanoscale,* vol. 4, pp. 1948-1963, 2012.

[18] E. J. Lopez-Naranjo, L. J. Gonzalez-Ortiz, L. M. Apatiga, E. M. Rivera-Munoz and A. Manzano-Ramirez, "Transparent Electrodes: A Review of the Use of Carbon-Based Nanomaterials," *Journal of Nanomaterials,* vol. 2016, p. 4928365, 2016.

[19] M. Kaempgen, G. Duesberg and S. Roth, "Transparent carbon nanotube coatings," *Applied Surface Science,* vol. 252, pp. 425-429, 2005.

[20] P. Levermore, L. Chen, X. Wang, R. Das and D. Bradley, "Fabrication of Highly Conductive Poly(3,4-ethylenedioxythiophene) Films by Vapor Phase Polymerization and Their Application in Efficient Organic Light-Emitting Diodes," *Advanced Materials,* vol. 19, no. 17, pp. 2379-2385, 2007.

[21] Y. Wen and J. Xu, "Scientific Importance of Water-Processable PEDOT:PSS and Preparation, Challenge and New Application in Sensors of Its Film Electrode: A Review," *Journal of Polymer Science Part A: Polymer Chemistry,* vol. 55, no. 7, pp. 1121-1150, 2017.

[22] P. Blake, P. D. Brimicombe, R. R. Nair, T. J. Booth, D. Jiang, F. Schedin, L. A. Ponomarenko, S. V. Morozov, H. F. Gleeson, E. W. Hill, A. K. Geim and K. S. Novoselov, "Graphene-Based Liquid Crystal Device," *Nano Letters,* vol. 8, no. 6, pp. 1704-1708, 2008.

[23] J. Wu, H. A. Becerril, Z. Bao, Z. Liu, Y. Chen and P. Peumans, "Organic solar cells with solution-processed graphene transparent electrodes," *Applied Physics Letters,* vol. 92, p. 263302, 2008.

[24]   X. Ho and H. Lu, "Electrical and optical properties of hybrid transparent electrodes that use metal grids and graphene films," *Journal of Materials Research,* vol. 28, no. 4, pp. 620-626, 2012.

[25]   J. Hong, J. Yeo, G. Kim, D. Kim, H. Lee, J. Kwon, H. Lee, P. Lee and S. H. Ko, "Nonvacuum, maskless fabrication of a flexible metal grid transparent conductor by low-temperature selective laser sintering of nanoparticle ink," *ACS Nano,* vol. 7, no. 6, pp. 5024-5031, 2013.

[26]   J. van de Groep, P. Spinelli and A. Polman, "Transparent Conducting Silver Nanowire Networks," *Nano Letters,* vol. 12, no. 6, pp. 3138-3144, 2012.

[27]   Y. Sun, B. Gates, B. Mayers and Y. Xia, "Crystalline Silver Nanowires by Soft Solution Processing," *Nano Letters,* vol. 2, no. 2, pp. 165-168, 2002.

[28]   C. Preston, Z. Fang, J. Murray, H. Zhu, J. Dai, J. N. Munday and L. Hu, "Silver nanowire transparent conducting paper- based electrode with high optical haze," *Journal of Materials Chemistry C,* vol. 2, pp. 1248-1254, 2014.

[29]   C. J. Emmott, A. Urbina and J. Nelson, "Environmental and economic assessment of ITO-free electrodes for organic solar cells," *Solar Energy Materials and Solar Cells,* vol. 97, pp. 14-21, 2012.

[30]   J.-Y. Lee, S. T. Connor, Y. Cui and P. Peumans, "Solution-Processed Metal Nanowire Mesh Transparent Electrodes," *Nano Letters,* vol. 8, no. 2, pp. 689-692, 2008.

[31]   S. De and J. N. Coleman, "The effects of percolation in nanostructured transparent conductors," *MRS Bulletin,* vol. 36, pp. 774-781, 2011.

[32]   L. Yang, T. Zhang, H. Zhou, S. C. Price, B. J. Wiley and W. You, "Solution-Processed Flexible Polymer Solar Cells with Silver Nanowire Electrodes," *Applied Materials and Interfaces,* vol. 3, no. 10, pp. 4075-4084, 2011.

[33]   H.-S. Kim, M. Patel, H.-H. Park, A. Ray, C. Jeong and J. Kim, "Thermally Stable Silver Nanowires-Embedding Metal Oxide for Schottky Junction Solar Cell," *Applied Materials and Interfaces,* vol. 8, no. 13, pp. 8662-8669, 2016.

[34]   J.-Y. Lee, S. T. Connor, Y. Cui and P. Peumans, "Semitransparent Organic Photovoltaic Cells with Laminated Top Electrode," *Nano Letters,* vol. 10, no. 4, pp. 1276-1279, 2010.

[35]   W. Gaynor, J.-Y. Lee and P. Peumans, "Fully Solution-Processed Inverted Polymer Solar Cells with Laminated Nanowire Electrodes," *ACS Nano,* vol. 4, no. 1, pp. 30-34, 2010.

[36]   T. Kim, Y. W. Kim, H. S. Lee, H. Kim, W. S. Yang and K. S. Suh, "Uniformly Interconnected Silver-Nanowire Networks for Transparent Film Heaters," *Advanced Functional Materials,* vol. 23, pp. 1250-1255, 2013.

[37] X.-Y. Zeng, Q.-K. Zhang, R.-M. Yu and C.-Z. Lu, "A New Transparent Conductor: Silver Nanowire Film Buried at the Surface of a Transparent Polymer," *Advanced Materials,* vol. 22, pp. 4484-4488, 2010.

[38] Z. Yu, Q. Zhang, L. Li, Q. Chen, X. Niu, J. Liu and Q. Pei, "Highly Flexible Silver Nanowire Electrodes for Shape-Memory Polymer Light-Emitting Diodes," *Advanced Materials,* vol. 23, pp. 664-668, 2011.

[39] L. Li, Z. Yu, W. Hu, C.-h. Chang, Q. Chen and Q. Pei, "Efficient Flexible Phosphorescent Polymer Light-Emitting Diodes Based on Silver Nanowire-Polymer Composite Electrode," *Advanced Materials,* vol. 23, pp. 5563-5567, 2011.

[40] W. Hu, X. Niu, R. Zhao and Q. Pei, "Elastomeric transparent capacitive sensors based on an interpenetrating composite of silver nanowires and polyurethane," *Applied Physics Letters,* vol. 083303, p. 102, 2013.

[41] H. H. Khaligh, K. Liew, Y. Han, N. M. Abukhdeir and I. A. Goldthorpe, "Silver nanowire transparent electrodes for liquid crystal-based smart windows," *Solar Energy Materials and Solar Cells,* vol. 132, pp. 337-341, 2015.

[42] M. Amjadi, A. Pichitpajongkit, S. Lee, S. Ryu and I. Park, "Highly Stretchable and Sensitive Strain Sensor Based on Silver Nanowire-Elastomer Nanocomposite," *ACS Nano,* vol. 8, no. 5, pp. 5154-5163, 2014.

[43] J. Wang, J. Jiu, M. Nogi, T. Sugahara, N. Shijo, H. Koga, P. He and K. Suganuma, "A highly sensitive and flexible pressure sensor with electrodes and elastomeric interlayer cotaining silver nanowires," *Nanoscale,* vol. 7, p. 2926, 2015.

[44] L. Xu, Y. Hou, M. Zhang, T. Cheng, W. Huang, C. Yao and Q. Wu, "Electrochemical sensor based on a silver nanowire modified electrode for the determination of cholesterol," *Analytical Methods,* vol. 5649, p. 7, 2015.

[45] J. Cui and Y. Liu, "Preparation of graphene oxide with silver nanowires to enhance antibacterial properties and cell compatibility," *RSC Advances,* vol. 5, no. 104, pp. 85748-85755, 2015.

[46] M. Polivkova, T. Hubacek, M. Staszek, V. Svorcik and J. Siegel, "Antimicrobial treatment of polymeric medical devices by silver nanomaterials and related technology," *International Journal of Molecular Sciences,* vol. 18, p. 419, 2017.

[47] Y. Chen, W. Lan, J. Wang, R. Zhu, Z. Yang, D. Ding, G. Tang, K. Wang, Q. Su and E. Xie, "Highly flexible, transparent, conductive and antibacterial films made of spin-coated silver nanowires and a protective ZnO layer," *Physica E,* vol. 76, pp. 88-94, 2016.

[48] T. Rai, P. Dantes, B. Bahreyni and W. S. Kim, "A Strechable RF Antenna With Silver Nanowires," *IEEE Electron Device LEtters,* vol. 34, no. 4, pp. 0741-3106, 2013.

[49] G.-W. Huang, H.-M. Xiao and S.-Y. Fu, "Wearable Electronics of Silver-Nanowire/Poly(dimethylsiloxane) Nanocomposite for Smart Clothing," *Scientific Reports,* vol. 5, p. 13971, 2015.

[50] M. R. Nateghi and M. Shateri--Khalilabad, "Silver nanowire-functionalized cotton fabric," *Carbohydrate Polymers,* vol. 117, pp. 160-168, 2015.

[51] D. Doganay, S. Coskun, S. P. Genlik and H. E. Unalan, "Silver nanowire decorated heatable textiles," *Nanotechnology,* vol. 27, no. 43, pp. 0957-4484, 2016.

[52] G.-W. Huang, H.-M. Xiao and S.-Y. Fu, "Wearable Electronics of Silver Nanowire/Poly(dimethylsiloxane) Nanocomposite for Smart Clothing," *Scientific Reports,* vol. 5, no. 13971, pp. 1-9, 2015.

[53] Y. Atwa, N. Maheshwari and I. A. Goldthorpe, "Silver nanowire coated threads for electrically conductive textiles," *Journal of Materials Chemistry C,* vol. 3, p. 3098, 2015.

[54] L. Shen, L. Du, S. Tan, Z. Zang, C. Zhao and W. Mai, "Flexible electrochromic supercapacitor hybrid electrodes based on tungsten oxide films and silver nanowires," *Chemical Communications,* vol. 52, pp. 6296-6299, 2016.

[55] C. Yan, W. Kang, J. Wang, M. Cui, X. Wang, C. Y. Foo, K. J. Chee and P. S. Lee, "Stretchable and Wearable Electrochromic Devices," *ACS Nano,* vol. 8, no. 1, pp. 316-322, 2014.

[56] R. Yuksel, S. Coskun, G. Gunbas, A. Cirpan, L. Toppare and H. E. Unalan, "Silver Nanowire/Conducting Polymer Nanocomposite Electrochromic Supercapacitor Electrodes," *Journal of The Electrochemical Society,* vol. 164, no. 4, pp. A721-A727, 2017.

[57] O. Ergun, S. Coskun, Y. Yusufoglu and H. E. Unalan, "High-performance, bare silver nanowire network transparent heaters," *Nanotechnology,* vol. 27, p. 445708, 2016.

[58] X. He, A. Liu, X. Hu, M. Song, F. Duan, Q. Lan, J. Xiao, J. Liu, M. Zhang, Y. Chen and Q. Zeng, "Temperature-controlled transparent-film heater based on silver nanowire- PMMA composite film," *Nanotechnology,* vol. 27, p. 475709, 2016.

[59] Y. Sun, B. Mayers, T. Herricks and Y. Xia, "Polyol Synthesis of Uniform Silver Nanowires: A Plausible Growth Mechanism and the Supporting Evidence," *Nano Letters,* vol. 3, no. 7, pp. 955-960, 2003.

[60] S. Coskun, B. ksoy and H. E. Unalan, "Polyol Synthesis of Silver Nanowires: An Extensive Parametric Study," *Crystal Growth and Design,* vol. 11, pp. 4963-4969, 2011.

[61] Z. Zhang, B. Zhao and L. Hu, "PVP Protective Mechanism of Ultrafine Silver Powder Synthesized by Chemical Reduction PRocesses," *Journal of Solid State Chemistry,* vol. 121, pp. 105-110, 1996.

[62] H. H. Khaligh and I. A. Goldthorpe, "Hot-rolling nanowire transparent electrodes for surface roughness minimization," *Nano Express,* vol. 9, no. 1, p. 310, 2014.

[63] H. H. Khaligh and I. A. Goldthorpe, "Failure of silver nanowire transparent electrodes under current flow," *Nanoscale,* vol. 8, no. 1, p. 235, 2013.

[64] J. L. Elechiguerra, L. Larios-Lopez, C. Liu, D. Garcia-Gutierrez, A. Camacho-Bragado and M. J. Yacaman, "Corrosion at the Nanoscale: The Case of Silver Nanowires and Nanoparticles," *Chemistry of Materials,* vol. 17, no. 24, pp. 6042-6052, 2005.

[65] J. Jiu, J. Wang, T. Sugahara, S. Nagao, M. Nogi, H. Koga, K. Suganuma, M. Hara, E. Nakazawa and H. Uchida, "The effect of light and himidity on the stability of silver nanowire transparent electrodes," *RSC Advances,* vol. 5, pp. 27657-27664, 2015.

[66] M. Lagrange, T. Sannicolo, Munoz-Rojas, B. Guillo Lohan, A. Khan, M. Anikin, C. Jiménez, F. Bruckert, Y. Bréchet and D. Bellet, "Understanding the mechanisms leading to failure in metallic nanowire-based transparent heaters, and solution for stability enhancement," *Nanotechnology,* vol. 28, p. 055709, 2017.

[67] C. Mayousse, C. Celle, A. Fraczkiewicz and J.-P. Simonato, "Stability of silver nanowire based electrodes under environmental and electrical stresses," *Nanoscale,* vol. 7, pp. 2107-2115, 2015.

[68] J. Jiu, J. Wang, T. Sugahara, S. Nagao, M. Nogi, H. Koga, K. Suganuma, M. Hara, E. Nakazawa and H. Uchida, "The effect of light and humidity on the stability of silver nanowire transparent electrodes," *RSC Advances,* vol. 5, pp. 27657-27664, 2015.

[69] I. K. Moon, J. I. Kim, H. Lee, K. Hur, W. C. Kim and H. Lee, "2D Graphene Oxide Nanosheets as an Adhesive Over-Coating Layer for Flexible Transparent Conductive Electrodes," *Scientific Reports,* vol. 3, no. 1112, pp. 1-7, 2012.

[70] J. Franey, G. Kammlott and T. Graedel, "The Corrosion of Silver by Atmospheric Sulfurous Gases," *Corrosion Science,* vol. 25, no. 2, pp. 133-143, 1985.

[71] H. Bennett, R. Peck, D. Burge and J. Bennett, "Formation and Growth of Tarnish on Evaporated Silver Films," *Journal of Applied Physics,* vol. 40, no. 8, pp. 3351-3360, 1969.

[72] B. H. Chudnovsky, "Degradation of Power Contacts in Industrial Atmosphere: Silver Corrosion and Whiskers," in *Reprinted from Proceedings of the Forty-Eighth IEEE Holm Conference on Electrical Contacts*, Orlando, 2002.

[73] R. Bauer, "Sulfide Corrosion of Silver Contacts During Sattelite Storage," Space Division- Air Force Systems Command, Los Angeles, 1988.

[74] B. Vaagensmith and Q. Qiao, "Effect of Synthesis Temperature, UV-Ozone Treatment, and Nanowire Diameter on the Failure of Silver Nanowire Electrodes," *IEEE Journal of Photovoltaics,* vol. 6, no. 6, pp. 1549-1553, 2016.

[75] H. L. Eom, J. Lee, A. Pichitpajongkit, M. Amjadi, J.-H. Jeong, E. Lee, J.-Y. Lee and I. Park, "Ag@Ni Core–Shell Nanowire Network for Robust Transparent Electrodes Against Oxidation and Sulfurization," *Small,* vol. 10, no. 20, pp. 4171-4181, 2014.

[76] D. G. Lee, D. Lee, S. Lee and H. S. Jung, "Effective passivation of Ag nanowire-based flexible transparent conducting electrode by TiO2 nanoshell," *Nano Convergence,* p. 3:20, 2016.

[77] A. Kim, Y. Won, K. Woo, C.-H. Kim and J. Moon, "Highly Transparent Low Resistance ZnO/Ag Nanowire/ZnO Composite Electrode for Thin Film Solar Cells," *ACS Nano,* vol. 7, no. 2, pp. 1081-1091, 2013.

[78] D. Lee, H. Lee, Y. Ahn, Y. Jeong, D.-Y. Lee and Y. Lee, "Highly stable and flexible silver nanowire-graphene hybrid transparent conducting electrodes for emerginc optoelectronic devices," *Nanoscale,* vol. 5, pp. 7750-7755, 2013.

[79] I. K. Moon, J. I. Kim, H. Lee, K. Hur, W. C. Kim and H. Lee, "2D Graphene Oxide Nanosheets as an Adhesive Over-Coating Layer for Flexible Transparent Conductive Electrodes," *Nature- Scientific Reports,* vol. 3, no. 12, pp. 1-7, 2012.

[80] J. S. Woo, j. T. Han, S. Jung, J. I. Jang, H. Y. Kim, H. J. Jeong, S. Y. Jeong, K.-J. Baeg and G.-W. Lee, "Electricall Robust Metal Nanowire Network Formation by In-Situ Interconnection with Single-Walled Carbon Nanotubes," *Scientific Reports,* vol. 4, p. 4084, 2014.

[81] C. Mayousse, C. Celle, A. Fraczkewicz and J.-P. Simonato, "Stability of silver nanowire based electrodes under environmental and electrical stresses," *Nanoscale,* vol. 7, pp. 2107-2115, 2015.

[82] M. Song, D. S. You, K. Lim, S. Park, S. Jung, C. S. Kim, D.-H. Kim, D.-G. Kim, J.-K. Kim, J. Park, Y.-C. Kang, J. Heo, S.-H. Jin, J. H. Park and J.-W. Kang, "Highly Effi cient and Bendable Organic Solar Cells with Solution-Processed Silver Nanowire Electrodes," *Advanced Functional Materials,* vol. 23, pp. 4177–4184, 2013.

[83] Z. Ding, V. Stoichkov, M. Horie, E. Brousseau and J. Kettle, "Spray coated silver nanowires as transparent electrodes in OPVs for Building Integrated Photovoltaics applications," *Solar Energy Materials and Solar Cells,* vol. 157, pp. 305-311, 2016.

[84]   F. Selzer, N. Weib, D. Kneppe, L. Bormann, C. Sachse, N. Gaponik, A. Eychmuller, K. Leo and L. Muller-Meskamp, "A spray-coating process for highly conductive silver nanowire networks as the transparent top-electrode for small molecule organic photovoltaics," *Nanoscale,* vol. 7, pp. 2777-2783, 2015.

[85]   W. Xiong, H. Liu, Y. Chen, M. Zheng, Y. Zhao, X. Kong, Y. Wang, X. Zhang, X. Kong, P. Wang and L. Jiang, "Highly Conductive, Air-Stable Silver Nanowire@Iongel Composite Films toward Flexible Transparent Electrodes," *Advanced Materials,* vol. 28, no. 33, pp. 7167-7172, 2016.

[86]   C.-H. Liu and X. Yu, "Silver nanowire-based transparent, flexible, and conductive thin film," *Nano Express,* vol. 6, p. 75, 2011.

[87]   Z. Li, C. Yang and R. Wang, "High Performance Silver Nanowire based Transparent Electrodes Reinforced by EVA Resin Adhesive," *IEEE Explore,* vol. 17, pp. 195-199, 2016.

[88]   H. Sim, S. Bok, B. Kim, M. Kim, G.-H. Lim, S. M. Cho and B. Lim, "Organic-Stabilizer-Free Polyol Synthesis of Silver Nanowires for Electrode Applications," *Angewandte Chemie International Edition,* vol. 55, no. 39, pp. 11814-11818, 2016.

[89]   L. Hu, H. S. Kim, J.-Y. Lee, P. Peumans and Y. Cui, "Scalable Coating and Properties of Transparent, Flexible, Silver nanowire Electrodes," *ACS Nano,* vol. 4, no. 5, pp. 2955-2963, 2010.

[90]   A. A. Tracton, "Wire-Wound Rod Coating," in *Coatings Technology; Fundamentals, Testing, and Processing Techniques*, Boca Raton, Taylor and Francis Group, 2006, pp. 19-1-19-7.

[91]   C.-H. Liu and X. Yu, "Silver nanowire-based transparent, flexible, and conductive thin film," *Nanoscale Research Letters,* vol. 6, p. 75, 2011.

[92]   D. P. Langley, M. Lagrange, C. Jiménez, G. Giusti, Y. Bréchet, N. Nguyen and D. Bellet, "Metallic nanowire networks: effects of thermal annealing on electrical resistance," *Nanoscale,* vol. 6, p. 135355, 2014.

[93]   H. H. Khaligh and I. A. Goldthorpe, "Hot-rolling nanowire transparent electrodes for surface roughness minimization," *Nanoscale Research Letters,* vol. 9, p. 310, 2014.

[94]   J.-Y. Lee, S. T. Connor, Y. Cui and P. Peumans, "Solution-Processed Metal Nanowire Mesh Transparent Electrodes," *Nano Letters,* vol. 8, no. 2, pp. 689-692, 2008.

[95]   S. B. Sepulveda-Mora and S. G. Cloutier, "Figures of Merit for High-Performance Transparent Electrodes Using Dip-Coated Silver Nanowire Networks," *Journal of Nanomaterials,* vol. 2012, p. 7, 2012.

[96]   A. Popelka, I. Krupa, I. Novak, M. A. S. A. Al-Maadeed and M. Ouederni, "Improvement of

aluminum/polyethylene adhesion through corona discharge," *Journal of Physics D: Applied Physics,* vol. 50, no. 3, p. 035204, 2016.

[97] A. Schutze, J. Y. Jeong, S. E. Babayan, J. Park, G. S. Selwyn and R. F. Hicks, "The Atmospheric-Pressure Plasma Jet: A Review and Comparison to Other Plasma Sources," *IEEE Transactions on Plasma Science,* vol. 26, no. 6, pp. 1685-1694, 1998.

[98] R. Gupta, "Silver nanowire electrodes: enabling flexible, transparent and cost effective OLED lighting," in *DOE SSL R&D Workshop*, San Francisco, 2015.

[99] J. Lucas, "What is Visible Light?," Live Science, 30 April 2015. [Online]. Available: http://www.livescience.com/50678-visible-light.html. [Accessed 12 May 2017].

[100] "Poly Print," Poly Print- Custom Printers and Laminators of Flexible Packaging, 2008. [Online]. Available: http://www.polyprint.com/flexographic-haze.htm. [Accessed 12 May 2017].

[101] G. Deignan and I. A. Goldthorpe, "The dependence of silver nanowire stability on network composition and processing parameters," *RSC Advances,* vol. 7, pp. 35590-35597, 2017.

[102] W. A. Saidi, H. Feng and K. A. Fichthorn, "Binding of Polyvinylpyrrolidone to Ag Surfaces: Insight into a Structure-Directing Agent from Dispersion-Corrected Density Functional Theory," *Journal of Physical Chemistry,* vol. 117, pp. 1163-1171, 212.

[103] S. Karim, M. Toimil-Molares, A. Balogh, W. Ensinger, T. Cornelius, E. Khan and R. Neumann, "Morphological evolution of Au nanowires controlled by Rayleigh instability," *Nanotechnology,* vol. 17, no. 24, pp. 5954-5959, 2006.

[104] J. Franey, G. Kammlott and T. Graedel, "The corrosion of silver by atmospheric sulfurous gases," *Corrosion Science,* vol. 25, no. 2, pp. 133-143, 1985.

[105] Y. Yuan and T. R. Lee, "Contact Angle and Wetting Properties," in *Surface Science Techniques*, Berlin, Springer-Verlag, 2013, pp. 3-34.

[106] A. Czanderna, "The Adsorption of Oxygen on Silver," *Journal of Physical Chemistry,* vol. 68, no. 10, pp. 2765-2771, 1964.

[107] R. Hoffmann and D. Turnbull, "Lattice and Grain Boundary Self-Diffusion in Silver," *Journal of Applied Physics,* vol. 22, no. 5, pp. 634-639, 1951.

[108] C. Tomizuka and E. Sonder, "Self-Diffusion in Silver*," *Physical Review,* vol. 103, no. 5, pp. 1182-1184, 1956.

[109] E. Marzbanrad, G. Rivers, P. Peng, B. Zhao and N. Y. Zhou, "How morphology and surface crystal

texture affect thermal stability of a metallic nanoparticle: the case of silver nanobelts and pentagonal silver nanowires," *Physical Chemistry Chemical Physics,* vol. 17, pp. 315-324, 2015.

[110] J. L. Elechiguerra, L. Larios-Lopez, C. Liu, D. Garcia-Gutierrez, A. Camacho-Bragado and M. J. Yacaman, "Corrosion at the Nanoscale: The Case of Silver Nanowires and Nanoparticles," *Chemistry of Materials,* vol. 17, pp. 6042-6052, 2005.

[111] J. H. Lee, P. Lee, D. Lee, S. S. Lee and S. H. Ko, "Large-Scale Synthesis and Characterization of Very Long Silver Nanowires via Successive Multistep Growth," *Crystal Growth and Design,* vol. 12, pp. 5598-5605, 2012.

[112] R. Jarrett and R. Crook, "Silver nanowire purification and separation by size and shape using multi-pass filtration," *Materials Research Innovations,* vol. 20, no. 2, pp. 86-91, 2016.

[113] D. Langley, M. Lagrange, C. Jiménez, G. Giusti, Y. Bréchet, N. Nguyen and D. Bellet, "Metallic nanowire networks: effects of thermal annealing on electrical resistance," *Nanoscale,* vol. 6, p. 135355, 2014.

[114] S. Karim, M. Toimil-Molares, W. Ensinger, A. Balogh, T. Cornelius, E. Khan and R. Neumann, "Influence of crystallinity on the Rayleigh instability of gold nanowires," *Journal of Physics D: Applied Physics,* vol. 40, no. 12, p. 3767, 2007.

[115] E. C. Garnett, W. Cai, J. J. Cha, F. Mahmood, S. T. Connor, M. G. Christoforo, Y. Cui, M. D. McGehee and M. L. Brongersma, "Self-limited plasmonic welding of silver nanowire junctions," *Nature Materials,* vol. 11, pp. 241-249, 2012.

[116] A. Volk, D. Knez, P. Thaler, A. W. Hauser, W. Grogger, F. Hofer and W. E. Ernst, "Thermal instabilities and Rayleight breakup of ultrathin silver nanowires grown in helium nanodroplets," *Phys.Chem.Chem.Phys,* vol. 17, pp. 24570-24575, 2015.

[117] H. Oh, J. Lee, J.-H. Kim, J.-W. Park and M. Lee, "Fabrication of Invisible Ag Nanowire Electrode Patterns Based on Laser-Induced Rayleigh Instability," *The Journal of Physical Chemistry,* vol. 120, pp. 20471-20477, 2016.

[118] X. Yu, X. Yu, J. Zhang, D. Zhang, J. Ni, H. Cai, D. Zhang and Y. Zhao, "Investigation of light transmission and scattering properties in silver nanowire mesh transparent electrodes," *Materials Letters,* vol. 145, pp. 219-223, 2015.

[119] M. Losurdo, I. Bergmair, M. M. Giangregorio, B. Dastmalchi, G. V. Bianco, C. Helgert, E. Pshenay-Severin, M. Falkner, T. Pertsch, E.-B. Kley, U. Huebner, M. A. Verschuuren, M. Muehlberger, K. Hingerl and G. Bruno, "Enhancing Chemical and Optical Stability of Silver Nanostructures by Low-Temperature Hydrogen Atoms Processing," *Journal of Physical Chemistry,* vol. 116, pp. 23004-

23012, 2012.

[120] S. D. Standridge, G. C. Schatz and J. T. Hupp, "Distance Depedence of Plasmon-Enhanced Photocurrent in Dye-Sensitized Solar Cells," *Journal of the American Chemical Society Communications,* vol. 131, pp. 8407-8409, 2009.

[121] D. Chanda, K. Shigeta, S. Gupta, T. Cain, A. Carlson, A. Mihi, A. J. Baca, G. R. Bogart, P. Braun and J. A. Rogers, "Large-area flexible 3D optical negative index metamaterial formed by nanotransfer printing," *Nature Nanotechnology,* vol. 6, pp. 402-407, 2011.

[122] T. Graedel, "Corrosion Mechanisms for Silver Exposed to the Atmosphere," *Journal of Electrochemistry,* vol. 139, no. 7, pp. 1963-1970, 1992.

[123] Y. Sun, B. Gates, B. Mayers and Y. Xia, "Crystalline Silver Nanowires by Soft Solution Processing," *Nano Letters,* vol. 2, no. 2, pp. 165-168, 2002.

[124] S. Coskun, B. Aksoy and H. E. Unalan, "Polyol Synthesis of Silver Nanowires: An Extensive Parametric Study," *Crystal Growth and Design,* vol. 11, pp. 4693-4699, 2011.

[125] X. M. Zeng, G. P. Martin and C. Marriott, "Effects of molecular weight of polyvinylpyrrolidone on the glass transition and crystallization of co-lyophilized sucrose," *International Journal of Pharmaceuticals,* vol. 218, no. 1-2, pp. 63-73, 2001.

[126] K. Gotoh, A. Yasukawa and Y. Kobayashi, "Wettability characteristics of poly(ethylene terephthalate) films treated by atmospheric pressure plasma and ultraviolet excimer light," *Polymer Journal,* vol. 43, pp. 545-551, 2011.

[127] R. A. Wolf, "Sample Chapter 2: Primary Polymer Adhesion Issues with Inks, Coatings, and Adhesives," in *Plastic Surface Modification: Surface Treatment and Adhesion*, Cincinnati, Hanser, 2010, pp. 3-12.

[128] T. Tokuno, M. Nogi, M. Karakawa, J. Jiu, T. T. Nge, Y. Aso and K. Suganuma, "Fabrication of silver nanowire transparent electrodes at room temperature," *Nano Research,* vol. 4, no. 12, pp. 1215-1222, 2011.

[129] H. M. Yates, L. A. Brook and D. W. Sheel, "Photoactive Thin Silver Films by Atmospheric Pressure CVD," *International Journal of Photoenergy,* vol. 2008, p. 870392, 2008.

[130] Y. Jin, D. Deng, Y. Cheng, L. Kong and F. Xiao, "Annealing-free and strongly adhesive silver nanowire networks with long-term reliability by introduction of a nonconductive and biocompatible polymer binder," *Nanoscale,* vol. 6, pp. 4812-4818, 2014.

[131] S. Aggarwal, M. F. van Hest, J. D. Perkins and D. S. Ginley, "Improving Mechanical Stability and

Electrical Properties of Silver Nanowire Films with a Zinc Tin Oxide Overcoat," *IEEE,* vol. 14, pp. 1022-1026, 2014.

[132] A. Kim, Y. Won, K. Woo, C.-H. Kim and J. Moon, "Highly Transparent Low Resistance ZnO/Ag Nanowire/ ZnO Composite Electrode for Thin Film SOlar Cells," *ACS Nano,* vol. 7, no. 2, pp. 1081-1091, 2013.

[133] F. Morgenstern, D. Kabra, S. Massip, T. J. Brenner, P. E. Lyons, J. N. Coleman and R. H. Friend, "Ag-nanowire films coated with ZnO nanoparticles as a transparent electrode for solar cells," *Applied Physics Letters,* vol. 99, p. 183307, 2011.

[134] P. Ramasamy, D.-M. Seo, S.-H. Kim and J. Kim, "Effects of TiO2 shells on optical and thermal properties of silver nanowires," *Journal of Materials Chemistry,* vol. 2012, p. 11651, 2012.

[135] J. Wang, J. Jiu, T. Sugahara, S. Nagao, M. Nogi, H. Koga, P. He, K. Suganuma and H. Uchida, "Highly Reliable Silver Nanowire Transparent Electrode Employing Selectively Patterned Barrier Shaped by Self-Masked Photolithography," *Applied Materials and Interfaces,* vol. 7, pp. 23297-23304, 2015.

[136] B. Wessling, "Passivation of Metals by Coating with Polyaniline: Corrosion Potential Shift and Morphological Changes," *Advanced Materials Communications,* vol. 6, no. 3, pp. 226-228, 1994.

[137] J. R. Santos , L. Mattoso and A. Motheo, "Investigation of corrosion protection of steel by polyaniline films," *Electrochimica Acta,* vol. 43, no. 3-4, pp. 309-313, 1998.

[138] D. E. Tallman, G. Spinks, A. Dominis and G. G. Wallace, "Electroactive conducting polymers for corrosion control," *Journal of Solid State Electrochemistry,* vol. 6, no. 2, pp. 73-84, 2002.

[139] A. Talo, O. Forsen and S. Ylassarri, "Corrosion protective polyaniline epoxy blend coatings on mild steel," *Synthetic Materials,* vol. 102, no. 1-3, pp. 1394-1395, 1999.

[140] T. Schauer, H. Greisiger and C. Eisenbach, "Corrosion protection of mild steel with polyaniline," *Polymer Preprints,* vol. 41, p. 1783, 2000.

[141] L. Shreir, R. Jarman and G. Burstein, Corrosion (3rd Edition) Volumes 1-2, Elsevier, 2003.

[142] M. T. Greiner and M. K. Festin, "Investigation of Corrosion-Inhibiting Aniline Oligomer Thin Films on Iron Using Photoelectron Spectroscopy," *Journal of Physical Chemistry,* vol. 112, pp. 18991-19004, 2008.

[143] A. Mohtasebi, T. Chowdhury, L. H. Hsu, M. C. Biesinger and P. Kruse, "Interfacial Charge Transfer between Phenyl-Capped Aniline Tetramer Films and Iron Oxide Surfaces," *Journal of Physical Chemistry C,* vol. 120, no. 51, pp. 29248-29263, 2016.

[144] B. Valdez, M. Schorr, R. Zlatev, M. Carrillo, M. Stoytcheva, L. Alvarez, A. Eliezer and N. Rosas, "Corrosion Control in Industry," in *Environmental and Industrial Corrosion- Practial and Theoretical Aspects*, Intech, 2012, p. Chapter 2.

[145] A. Holt, M. Facciotti, P. Amaro, R. Brown, P. Lewin, J. Pilgrim, G. Wilson and P. Jarman, "An Initial Study into Silver Corrosion in Transformers Following Oil Reclamation," in *Electrical insulation Conference*, Ottawa, 2013.

[146] B. H. Chudnovsky, "Degradation of Power Contacts in Industrial Atmosphere: Silver Corrosion and Whiskers," in *IEEE Holm Conference on Electrical Contacts*, West Chester, 2002.

[147] J. Elechiguerra, L. Larios-Lopez, C. Liu, D. Garcia-Gutierrez, A. Camancho-Bragado and M. Yacaman, "Corrosion at the Nanoscale: The Case of Silver Nanowires and Nanoparticles," *Chemistry of Materials,* vol. 17, no. 24, pp. 6042-6052, 2005.

[148] C. Mayousse, C. Celle, A. Frazkiewicz and S. J.P., "Stability of silver nanowire based electrodes under environmental and electrical stresses," *Nanoscale,* vol. 7, pp. 2107-2115, 2015.

[149] A. R. Madaria, A. Kumar, F. N. Ishikawa and C. Zhou, "Uniform, Highly Conductive, and Patterned Transparent Films of a Percolating Silver Nanowire Network on Rigid and Flexible Substrates Using a Dry Transfer Technique," *Nano Research,* vol. 3, pp. 564-573, 2010.

[150] R. Zhu, C.-H. Chung, K. C. Cha, W. Yang, Y. B. Zheng, H. Zhou, T.-B. Song, C.-C. Chen, P. S. Weiss, G. Li and Y. Yang, "Fused Silver Nanowires with Metal Oxide Nanoparticles and Organic Polymers for Highly Transparent Conductors," *ACS Nano,* vol. 5, no. 12, pp. 9877-9882, 2011.

[151] J. Song, L. Wang, A. Zibart and C. Koch, "Corrosion Protection of Electrically Conductive Surfaces," *Metals,* vol. 2, pp. 450-477, 2012.

[152] B. H. Chudnovsky, "Degradation of Power Contacts in Industrial Atmosphere: Silver Corrosion and Whiskers," in *Proceedings of the Forty-Eighth IEEE Holm Conference on Electrical Contacts*, Orlando, 2002.

[153] S. Viennot, F. Dalard, M. Lissac and B. Grosgogeat, "Corrosion resistance of cobalt-chromium and palladium-silver alloys used in fixed prosthetic restorations," *European Journal of Oral sciences,* vol. 113, pp. 90-95, 2005.

[154] Adafruit, "ITO (Indium Tin Oxide) Coated Glass- 50mm x 50mm," Adafruit, 2016. [Online]. Available: https://www.adafruit.com/product/1310. [Accessed 9 March 2017].

[155] P. Bullen and R. Isele, "German flat panel display forum (DFF)," European Technology: Flat Panel Displays 6th edn, (Germany: VDMA), 2008.

[156] W. Wong Kromhout, "UCLA Engineers Create Tandem Polymer Solar Cells that set Record for Energy-Conversion," UCLA Engineering- Henry Samueli School of Engineering and Applied Science, Los Angeles, 2012.

[157] D. S. Hecht, L. Hu and G. Irvin, "Emerginc Transparent Electrodes Based on Thin Films of Carbon Nanotubes, Graphene, and Metallic Nanostructures," *Advanced Materials,* vol. 23, no. 13, pp. 1482-1513, 2011.

[158] C. J. Emmott, A. Urbina and J. Nelson, "Environmental and economic assessment of ITO-free electrodes for organic solar cells," *Solar Energy Materials and Solar Cells,* vol. 97, pp. 14-21, 2012.

[159] S. Iijima, "Helical microtubules of graphitic carbon," *Nature,* vol. 354, pp. 56-58, 1991.

[160] F. Mirri, A. W. Ma, T. T. Hsu, N. Behabtu, S. L. Eichmann, C. C. Young, D. E. Tsentalovich and M. Pasquali, "High-Performance Carbon Nanotube Transparent Conductive Films by Scalable Dip Coating," *ACS Nano,* vol. 6, no. 11, pp. 9737-9744, 2011.

[161] L. Hu, D. Hecht and G. Gruner, "Percolation in Transparent and Conducting Carbon Nanotube Networks," *Nano Letters,* vol. 4, no. 12, pp. 2513-2517, 2004.

[162] A. A. Green and M. C. Hersam, "Colored semitransparent conductive coatings consisting of monodisperse metallic single-walled carbon nanotubes," *Nano Letters,* vol. 8, no. 5, pp. 1417-1422, 2008.

[163] B. B. Parekh, G. Fanchini, G. Eda and M. Chhowalla, "Improved conductivity of transparent single-wall carbon nanotube thin films via stable postdeposition functionalization," *Applied Physics Letters,* vol. 90, no. 12, p. 121913, 2007.

[164] T. Sreekumar, T. Liu and S. Kumar, "Single-Wall Carbon Nanotube Films," *Chemistry of Materials,* vol. 15, pp. 175-178, 2003.

[165] Y. Zhou and R. Azumi, "Carbon nanotube based transparent conductive films: progress, challenges, and perspectives," *Science and Technology of Advanced Materials,* vol. 17, no. 1, pp. 493-516, 2016.

[166] M. Schmidt, A. Falco, M. Loch, P. Lugli and G. Scarpa, "Spray coated indium-tin-oxide-free organic photodiodes with PEDOT:PSS anodes," *AIP Advances,* vol. 4, no. 10, p. 107132, 2014.

[167] E. Ahlswede, W. Muhleisen, M. Wahinuddin bin Moh Wahi, J. Hanisch and M. Opwalla, "Highly efficient organic solar cells with printable low-cost transparent contacts," *Applied Physics Letters,* vol. 92, no. 14, p. 143307, 2008.

[168] H. Do, M. Reinhard, H. Vogeler, M. F. Puetz, W. Schabel, A. Colsmann and U. Lemmer, "Polymeric

anodes from poly(3,4-ethylenedioxythiophene):poly(styrenesulfonate) for 3.5% efficient organic solar cells," *Thin Solid Films,* vol. 517, no. 20, pp. 5900-5902, 2009.

[169] Y. Xu and J. Liu, "Graphene as Transparent Electrodes: Fabrication and New Emerging Applications," *Small,* vol. 12, no. 11, pp. 1400-1419, 2016.

[170] M. Buzaglo, M. Shtein, S. Kober, R. Lovrincic, A. Vilan and O. Regev, "Critical parameters in exfoliating graphite into graphene," *Physical Chemistry Chemical Physics,* vol. 15, pp. 4428-4335, 2013.

[171] J. Kang, D. Shin, S. Bae and B. H. Hong, "Graphene transfer: key for applications," *Nanoscale,* vol. 4, pp. 5527-5537, 2012.

[172] K.-Y. Shin and J. Jang, "Highly conductive, flexible and scalable graphene hybrid thin films with controlled domain size as transparent electrodes," *Chemical Communications,* vol. 50, pp. 6645-6648, 2014.

[173] N. Leavitt, "ClearOhm Silver Nanowires in Breakthrough Medical Application," Cambrios Advanced Materials, Sunnyvale, CA, 2015.

[174] J. Jiu, J. Wang, T. Sugahara, S. Nagao, M. Nogi, H. Koga, K. Suganuma, M. Hara, E. Nakazawa and H. Uchida, "The effect of light and humidity on the stability of silver nanowire transparent electrodes," *RSC Advances,* vol. 5, pp. 27657-27664, 2015.

[175] Z. Reimer, "SEM Lab- Silver Sulfide Growth," 26 January 2015. [Online]. Available: http://www.semlab.com/blog/?p=425. [Accessed 4 May 2017].

[176] S. Liu, S. Ho and F. So, "Novel Patterning Method for Silver Nanowire Electrodes for Thermal-Evaporated Organic Light Emitting Diodes," *Applied Materials and Interfaces,* vol. 8, pp. 9268-9274, 2016.

[177] A. A. Tracton, "Coatings Technology: Fundamentals, Testing, and Processing Techniques," in *Coatings Technology*, CRC Press, 2006, pp. 19-7.

[178] J. Ma and M. Zhan, "Rapid production of silver nanowires based on high concentration of AgNO3 precursor and hte use of FeCl3 as reaction promoter," *RSC Advances,* vol. 4, p. 21060, 2014.

[179] J. E. Jackson, "Cost of Corrosion Annually in the US Over $1.1 Trillion in 2016," G2MT Laboratories, 2017. [Online]. Available: http://www.g2mtlabs.com/corrosion/cost-of-corrosion/. [Accessed 16 June 2017].

[180] Y. We, H. Jamasb, S. Cheng and S. Jansen, "Corrosion protection properties of coatings of the aniline oligomers and their epoxy resin-cured derivatives based on salt spray and cyclic testing,"

American Chemical Society, Polymer Preprints, Division of Polymer Chemistry, vol. 41, pp. 1778-1779, 2000.

[181] C. Dalmolin, S. C. Canobre, S. R. Biaggio, R. C. Rocha-Filho and N. Bocchi, "Electropolymerization of polyaniline on high surface area carbon substrates," *Journal of Electroanalytical Chemistry,* vol. 578, pp. 9-15, 2005.

[182] D. A. Outka and R. Madix, "The adsorption of nitrogen dioxide on the Ag(110) surface and formation of a surface nitrate," *Surface Science,* vol. 179, no. 1, pp. 1-24, 1987.

[183] OSHA, "OSHA Fact Sheet- Hydrogen Sulfide (H2S)," OSHA, October 2005. [Online]. Available: https://www.osha.gov/OshDoc/data_Hurricane_Facts/hydrogen_sulfide_fact.pdf. [Accessed 16 June 2017].

[184] P.-C. Hsu, H. Wu, T. J. Carney, M. T. McDowell, Y. Yang, E. C. Garnett, M. Li, L. Hu and Y. Cui, "Passivation Coating on Electrospun Copper Nanofibers for Stable Transparent Electrodes," *ACS Nano,* vol. 6, no. 6, pp. 5150-5156, 2012.

[185] A. Kim, Y. Won, K. Woo, C.-H. Kim and J. Moon, "Highly Transparent Low Resistance ZnO/Ag Nanowire/ ZnO Composite Electrode for Thin Film Solar Cells," *ACS Nano,* vol. 7, no. 2, pp. 1081-1091, 2013.

[186] L. Donghwa, H. Lee, Y. Ahn, Y. Jeong, D.-Y. Lee and Y. Lee, "Highly stable and flexible silver nanowire-graphene hybrid transparent conducting electrodes for emerging optoelectronic devices," *Nanoscale,* vol. 5, pp. 7750-7755, 2013.

[187] J. Liang, L. Li, K. Tong, Z. Ren, W. Hu, X. Niu, Y. Chen and Q. Pei, "Silver nanowire percolation network soldered with graphene oxide at room temperature and its application for fully stretchable polymer light emitting diodes," *ACS Nano,* vol. 8, no. 2, pp. 1590-1600, 2014.

[188] F. S. F. Morgenstern, D. Kabra, S. Massip, T. J. Brenner, P. E. Lyons, J. N. Coleman and R. H. Friend, "Ag- nanowire films coated with ZnO nanoparticles as a transparent electrode for solar cells," *Applied Physics Letters,* vol. 183307, no. 99, 2011.

[189] P. Ramasamy, D.-M. Seo, S.-H. Kim and J. Kim, "Effects of TiO2 shells on optical and thermal properties of silver nanowires," *Journal of Materials Chemistry,* vol. 22, pp. 11651-11657, 2012.

[190] X.-Y. Zeng, Q.-K. Zhang, R.-M. Yu and C.-Z. Lu, "A New Transparent Conductor: Silver Nanowire Film Buried at the Surface of a Transparent Polymer," *Advanced Materials,* vol. 22, pp. 4484-4488, 2010.

[191] C. Yang, H. Gu, W. Lin, M. M. Yuen, C. P. Wong, M. Xiong and B. Gao, "Silver Nanwires: From Scalable Synthesis to Recyclable Foldable Electronics," *Advanced Materials,* vol. 23, pp. 3052-3056,

2011.

[192] M. Parpia, E. Tevaarwerk, N. A. Amro, R. Sanedrin, H.-T. Wang and J. Haaheim, "Dip Pen Nanolithography of Silver Nanoparticle-based Inks for Printed Electronics," *Nanotechnology,* vol. 1, pp. 654-657, 2008.